The biomechanical properties of the capsular and bursal layers of the rotator cuff complex: A clinical investigation

Submitted by: Martie Vosloo

A thesis submitted to the Department of Anatomy, School of Medicine, Faculty of Health Sciences, University of Pretoria, in the fulfilment of the requirements for the degree

Of

MSc in Anatomy

Pretoria 2018

Supervisor: Dr Natalie Keough

Co-supervisor: Prof R Mostert

DECLARATION

I, Martie Vosloo, declare that this thesis is my own work. It is being submitted for the degree of MSc/PhD in Anatomy at the University of Pretoria. It had not been submitted before for any other degree or examination at this or any other Institution.

Sign _____

The 13 Day of Sep., 2018

Table of Contents

List of Figures

List of Tables

Abstract

Studies have shown that the rotator cuff (RC) complex is not simply comprised out of four separate tendons inserting onto the tubercles of the humerus, but rather a far more complex, integrated and interconnected system. This system is comprised of multiple layers, each with a unique set of properties. Current surgical practice however, treats the RC tendons as one layer, which only focuses on the bursal/tendinous layer (superficial tendinous layer) during repair. The capsular layer, which lies deep to the bursal/tendinous layer is often overlooked and most often treated together with the bursal/tendinous layer during repair. This has led to multiple postoperative complications including high re-tear rates, tears in new places, limited movement and poor recovery. Therefore, the aim of this study was to investigate the biomechanical properties of healthy RC tendons (both capsular and tendinous layers) in a South African population.

The total sample studied was comprised of 17 fresh/frozen shoulder specimens and 5 cadaveric shoulders. Of the 17 fresh shoulders 7 right and 6 left were harvested from 9 white males and 2 right and 2 left from 2 white females. The mean age of the fresh sample was 64.6 years. The cadaveric shoulders, 1 was male (right = 1; left = 1) and 2 were female (right = 2; left = 1) with a mean age of 64.7 years. Tensile tests were performed on the selected RC tendons using a benchtop MTS Criterion Model 41 tensile testing machine for composite materials, fitted with a 1kN load cell. The tendons were secured with rubber soft tissue clamps and reinforced with sand paper. Each strip was tested to failure at a constant rate of 0.5 mm/s, recording results using the MTS Test suit TWE 4.1.5.736. Measurements included: peak load of each layer, in Newton force (N) and the modulus of elasticity, in megapascals (MPa).

The results for the peak load (N) value indicated significant differences between the cadaveric Supraspinatus SS layer and the bursal SS layer ($p=0.002$) and between the cadaveric Infraspinatus IS and bursal IS layer ($p=0.0003$). For the modulus (MPa) value, there were significant differences between the bursal IS and bursal Subscapular SC ($p=0.012$), as well as the bursal SS and bursal SC ($p=0.020$). With regard to the anisotropic nature of the tendons, the graphs gave a better indication of the layer's differences. The bursal/tendinous layer presented with higher flexibility than the capsular layer. The graphs illustrated that the bursal/tendinous layer's fibres parted separately during tensile testing, while the capsular layer broke more as a complete section. This corresponds with the more fibrous and cartilaginous properties in the capsular layer.

Therefore, looking at the results, it is evidence that the bursal/tendinous and capsular layer have different biomechanical properties, and that not only statistical values should be used, but a closer look should be taken at how these layers react physically as they experience load or strain. These results may have clinical implications in that surgeons should start to treat the two layers separately during surgical repair procedures.

Keywords

Biomechanical; rotator cuff; peak load; embalming; elasticity; fibrous; cartliginous; modulus; anisotropic; procedures.

Acknowledgements

The authors would like to acknowledge the families and the donors for their body donation to the Department of Anatomy in the School of Medicine as well as to the National Tissue Bank, without their contributions this study would not have been possible. The author would like to acknowledge Mrs M Pretorius for the graphic work done and presented in the project. The authors would also like to acknowledge Muhammed Yusuf Saloje for the assistance with regards to data presentation and interpretation together with Prof Roelf Mostert and Sibusiso Mahlalela at the Department of Material Sciences and Metallurgy at the University of Pretoria for assisting in the project. Another acknowledgement to the Department of Mechanical engineering at UNISA (Florida campus) for making the facility and equipment available to use during the study. I would also like to thank the RDP (Research Development program) from the University of Pretoria (UP), as well as the NRF (National Research Foundation) for funding this project. A specials thank you to Dr MA De Beer for the inspiration of this project and his clinical support during the project. Also to Dr Natalie Keough as co-author and supervisor that not only assisted, but inspired, motivated and contributed so much during this project. Lastly I would like to thank my husband JG Vosloo, family and friends for the support and encouragement. Without these people and facilities, none of this could be possible.

Chapter 1: Introduction

The biomechanical properties of the rotator cuff (RC) complex is defined as the mechanical function of the movement of the RC and how it is influenced by internal and external systems (www.dictionary.com, 2018). The study of biomechanical properties of the RC is often overlooked and, even more so, the importance of these properties and how they relate to the clinical/surgical field (Nakajima *et al.*, 1994; Chaudhury *et al*., 2011).

To investigate and plan a RC repair surgery, it is of vital importance to understand the function of the RC and which external and internal systems influence these mechanisms. Knowing, understanding and appreciating this information may lead to better and enhanced postoperative outcomes of the surgery such as, returning the shoulder to full mechanical function. Knowledge of the intricate nature of the mechanical aspects, as well as the complex anatomical layout of the RC complex may not always be the firstconcern for all surgeons. This lack of knowledge application often leads to severe postoperative complications after RC surgery, especially in the case of full-thickness repairs, and includes complications such as high re-tear rates, postarthroscopic humeral head necrosis, pain, and lack of full functionality and mobility. Understanding and applying the basic concepts of RC anatomy and biomechanics during repair surgery should be a non-negotiable practice for every Orthopaedic surgeon.

Over the last couple of decades studies have shown that the RC complex is not just as simple as four tendons inserting onto predefined sites on the tubercles of the humerus, but rather a far more complex, integrated and interconnected system comprised of multiple layers each with their own unique set of properties (Clark *et al.*, 1992; Nakajima *et al.*, 1994; Vosloo *et al*., 2017). It has been demonstrated that in fact, the tendons of the RC interdigitate with each other and instead of singular insertions onto the humerus they insert as a singular unit/cuff extending from the inferior aspect of the greater tubercle to the lowest insertion point on the lesser tubercle (Clark *et al*., 1992; Vosloo *et al.*, 2017). The current practice during surgery however, is to treat the RC tendons "separately" and only focus on the bursal/tendinous layer, which is the superficial tendinous layer during reattachment to the humeral tubercle (De Beer, *per comm*; Clark *et al.*, 1992; Adam *et al*., 2016). The capsular layer which lies deep to the bursal/tendinous layer is often ignored and treated together with the overlying bursal/tendinous layer. The bursal/tendinous layer and the capsular layer (aka: internal joint capsule) are interconnected and inseparable from each other about 1-2 cm proximal to their insertion onto the humerus. Although these layers appear inseparable at their insertion, they do have distinct mechanical properties, and this has been observed in surgical situations where these layers can tear dependently or independently from each other (De Beer, *pers comm*). Clark *et al.* (1992) and Nakajima *et al.* (1994) clearly demonstrated that these two layers display different biomechanical properties, with the tendinous layer being tougher, with higher elastic properties and the capsular layer being more fragile, with higher cartilaginous properties. Considering this fact, sparse research has been conducted on

these different layers and the surgical implications that this could have on the RC repair success. As previously mentioned, most surgeons only repair the bursal/tendinous part of the RC and either miss the injury to the capsular part or simply repair the capsular and bursal/tendinous layers together as one structure (De Beer, *per comm;* Adam *et al*., 2016*).*

According to De Beer (*Pers Comm*) and Adam et al. (2016), the capsular layer should also be restored to its normal anatomy separately from the bursal/tendinous layer to allow for proper recovery and better mechanical stability postoperatively. Considering the current arthroscopic re-tear rates 11% to 94%, (considering activity, tear size and age of patient) and complications observed postoperatively, it is clear that more high-quality, experimental research is required concerning the RC complex and its anatomical and biomechanical function. Therefore, the aim of this study was to investigate the biomechanical properties of the two layers, which includes the bursal/tendinous layer and the capsular layer.

Chapter 2: Literature Review

2.1 General

Rotator cuff (RC) repairs are identified as one of the most common surgeries, with up to 50% of the general population visiting practitioners due to shoulder pain (Chaudhury *et al*., 2011). RC repairs currently still result in controversial success rates, especially with regard to more modern arthroscopic techniques using suture anchors, which have shown failure rates of between 11% and 94% (Kim *et al*., 2006 Le *et al*., 2014; Ahmad *et al*., 2015). Not only do these procedures offer low success rates, but also indicates difficulties in areas such as: re-operations due to re-tears in the tendons, and high costs associated with suture anchors, shifting of the anchors, and knot impingement (Cummins and Murrell, 2003; Kuroda *et al*., 2013).

The most important aspect often overlooked in these surgeries, is the biomechanical integrity and postoperative maintenance of the RC, which in practice should be the primary goal of the surgeon; restoration of shoulder function to pre-injury levels. Surgeries using suture anchors have not only shown high percentages of re-tear rates, but also a decrease in shoulder function postoperatively (Cummins and Murrell, 2003). Numerous factors play a role in optimal repair and ultimate postoperative success of these torn tendons, including the correct tendon to bone contact, the bone and tendon tissue quality and, repairing the correct motion of the tendon to bone, which involves correct tendon footprint placement (Park *et al*., 2007). These factors are important not only during surgery, but also specifically, for better postoperative success and should be the focus of surgeons by using correct and optimal techniques to achieve these results. Aside from the evident possibility of re-tears resulting most often from the incorrect placement of tendon to bone and poor bone quality, there is also another factor to consider, namely the vascularisation of the RC tissue and bone. Avascular zones are known to be one of the primary reasons for degeneration and rupture of tendons and a lack of healing in these zones may cause hypo-vascularisation, which ultimately results in postoperative defects (Finwick *et al*., 2002).

To avoid these postoperative defects, it is important to clearly define and understand the anatomy of the RC for successful repairs and should be the surgeon's main objective.

2.2 Anatomy of the rotator cuff unit

Up to date knowledge and understanding of the correct anatomy should be considered most vital for successful RC repair surgery. RC tendons are still considered, and taught at tertiary level education (example: university and college), to have separate insertions onto the lesser and greater tubercles of the humerus. Despite this theory taught, RC repair outcomes are still highly unsuccessful (De Beer, *per comm;* Gerber *et al.*, 1994*;* Kim *et al*., 2006; Le *et al*., 2014; Ahmad *et al*., 2015; Adam *et al*., 2016*)*. Contradicting this understanding, is the

research that clearly demonstrates an interdigitation between the tendons, considering it more to be, and act as one unit with a common attachment onto the tubercles.

2.2.1 Insertion of the RC

The accepted definition for the insertion of the tendon of subscapularis (SC) is onto the lesser tubercle, tapering down towards the surgical neck of the humerus creating an auricular shape. Supraspinatus (SS) tendon inserts onto the highest impression of the greater tubercle creating a more triangular or trapezoidal shape. The tendon of infraspinatus (IS) inserts onto the middle impression of the greater tubercle, creating a trapezoidal shape and teres minor (TM) tendon inserts onto the lowest impression of the greater tubercle, tapering down onto the surgical neck, creating a triangular shape (Curtis *et al*., 2006; Mochizuki *et al*., 2008).

Due to these widespread and simplified classifications and definitions, the fact that the insertions of the RC tendons are more complex, of a singular and combined (interdigitated) nature is not often considered, and often misunderstood. Instead, the singular insertion zones can only be created and defined by forcefully separating tendinous attachments from each other by following the muscle borders, thus creating these pre-perceived shapes and classifying them as individual footprints. Despite further studies contradicting these findings, and demonstrating a more common and intertwined insertion onto the tubercles of the humerus, this complexity is still currently ignored in most anatomical and clinical settings. These findings not only reiterate the common, singular interconnected insertional area onto the tubercles, but also reveal an interdigitation between these tendons and the underlying internal joint capsule (Figure 2.1) (Clark *et al*., 1992; Pouliart and Gagey, 2006; Vosloo *et al*., 2017).

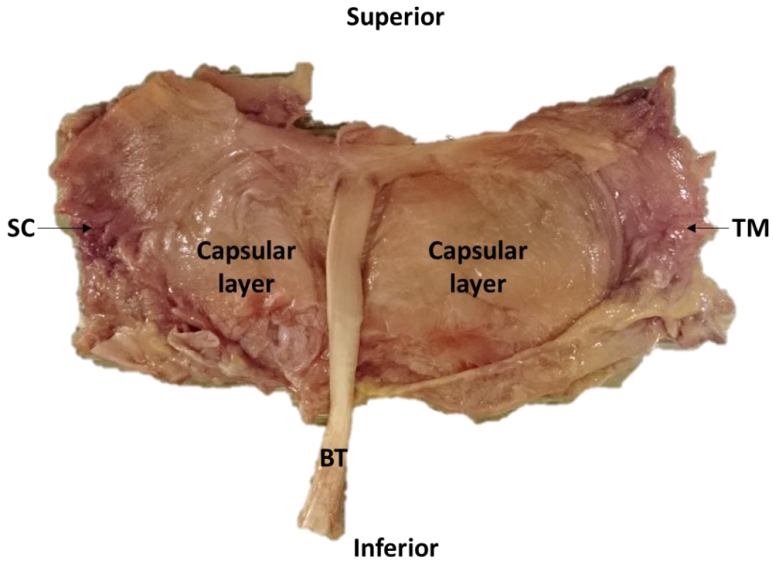

Figure 2.1. Internal view of the complete RC unit. Subscapularis (SC), teres minor (TM), long head of biceps (BT)

The prominent and clinically relevant interdigitation sites include the SC and SS along the more superior aspect of the bicipital groove (intertubercular groove), creating an extension hood over the long head of the biceps tendon. Another interdigitation is observed between IS and SS, being inseparable approximately 15mm proximal to their common insertion onto the greater tubercle (Clark *et al*., 1992; Pouliart and Gagey, 2006; Vosloo *et al*., 2017). The deeper layers of SS and IS fuse to the internal joint capsule of the glenohumeral joint (GHJ), highlighting the importance of the joint capsule/internal capsule (IC) in the biomechanical aspects of the repair; this should be considered during surgery for reinstating the normal biomechanical properties of the shoulder postoperatively (Vosloo *et al*., 2017). A study by Clark *et al*. (1992) showed that the RC unit consisted mainly out of 5 layers: fibres of the coracohumeral ligament (Layer 1); tendon fibres from the RC muscle tendons (Layer 2); tendinous structure in which fascicles are smaller and not uniform unlike those in layer 2 (Layer 3); loose connective tissue with thick collagen bands (Layer 4) and the IC of the glenohumeral joint (Layer 5). These layers are significant in the fact that they play a critical role in the biomechanical properties of the RC unit.

The 5 layers comprising the RC unit, interdigitate with one another and due to the difference in composition, the tensile strength differs across all tendons, making the RC unit a anisotropic material. This difference in tensile properties may cause one layer to tear before another or even in a different direction, specifically with regard to the IC, which can be overlooked and not often repaired. It is believed that the bursal/tendinous layer can handle more stress and strain when compared to the capsular layer and may have a higher level of elasticity allowing it to stretch up to three times longer than the capsule before tearing (De Beer, *Pers. Comm. 2016*). If the capsular layer is overlooked and not considered in the repair

method, it may potentially result in a new tear due to additional strain on the repaired tendon that now has to function alone under a compromised condition (Adam *et al*., 2016)

2.2.2 Vascular supply to the rotator cuff

Tendons are known to be poorly vascularised and therefore prone to injuries. Tendons depend mostly on synovial fluid diffusion for nourishment, which is regulated and controlled by the cardiovascular system. Vascularisation of the RC is important for sufficient perfusion providing the necessary factors for tissue healing and therefore, needs to be taken into consideration during RC surgeries (Fenwick *et al*., 2002).

The main arterial supply of the RC is made up of the ascending branch of the anterior circumflex humeral artery (ACHA), the suprascapular, posterior circumflex humeral arteries (PCHA) and the acromial branch of the thoracoacromial artery (Chansky and Iannotti, 1991; Naidoo *et al.,* 2014). The tendons receive blood supply from the muscular branches (Figure 2.2), as well as intraosseous branches from the dense anastomoses formed by the ascending branches of the PCHA and the ACHA. This anastomosis also gives blood supply to the joint capsule (Papakonstantinou *et al*., 2012). RC vascular studies suggest that an avascular zone, prominent in the SS tendon, is the main cause of degeneration of the aging tendon and the poor healing properties of the tendon postoperatively. (Ling *et al.*, 1990; Chansky and Iannotti, 1991) However, other studies have proposed that this zone is in fact a myth and if present, a minimal contributor, if at all, to cuff tears and degeneration (Goodmurphy *et al.*, 2003; Nho *et al*., 2008). A large gap still exists in the literature with regard to the blood supply of both the proximal humerus and RC unit and of the literature that is present, various contradictions and controversies exist. In the SC, IS and TM tendons it has been shown that a good vascular bed is present in these tendons (Rathbun and Macnab, 1970; Chansky and Iannotti, 1991). With regard to the actual relationship of the blood supply and surgical intervention, several studies have revealed a significant decrease in vascular scores after RC repair using anchor-sutures, with 48% of the patients having postoperative defects and the lowest vascular score at the anchor site. This may result in re-tear, weakness, pain and other indirect defects due to the unhealed RC tendon and damaged blood flow (Fealy *et al.*, 2006; Gamradt *et al*., 2010; Tham *et al*., 2013).

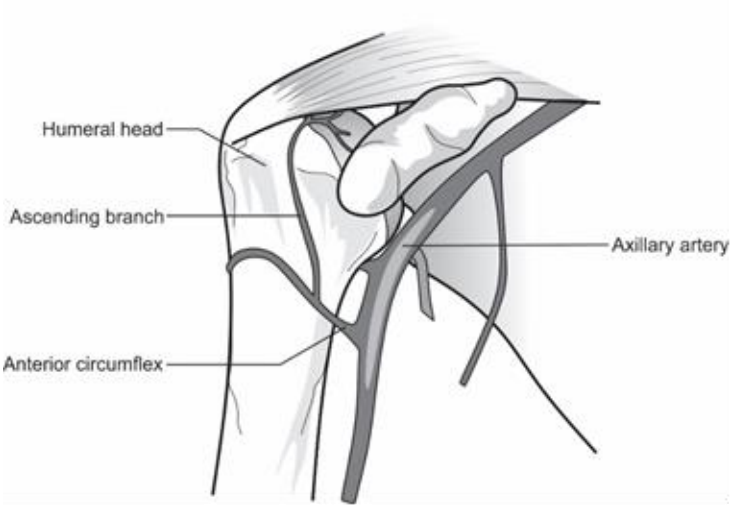

Figure 2.2. Anterior view, showing the blood supply of the humerus of RC (Hussey, Steen and Frankle, 2016)

To regularly, and theoretically stimulate vascular response of the healing tendon, the decortication of bone is performed at the repaired site, and even this procedure does not guarantee a better success postoperatively (Hegedus *et al*., 2009; Gamradt *et al*., 2010). Other stimulating approaches, such as exercise, is also used to increase blood flow after surgical repair. According to Gamradt et al. (2010), a 15% increase in blood flow in peri-bursal region and 50% in repaired region was recorded after exercise.

2.3 RC tears and surgical repair techniques

The use of classification systems to identify the type of tear is vital when considering the most appropriate treatments for each type of tear. There are several classification systems for RC tears and treatment modalities. Some include Snyder's and Ellman's classification, which is popular for partial thickness tears, others like DeOrio and Cofield classification and Bayne and Bateman classification system focus more on full thickness tears (Belangero *et al.*, 2013). Whether surgery is required or what type of surgical approach is used is often dependant on the surgeon involved. There is currently no consensus as to which treatment modality (surgery versus non-surgery) or surgical approach (arthroscopic versus open) is the best for the best postoperative outcomes.

2.3.1 Aetiology of RC tears

RC tears are caused by either degenerative or traumatic events, influenced by intrinsic and or extrinsic factors. Degenerative causes are known to be the most frequent reason for tears to occur, due to multiple factors, including age, overuse of shoulder and diseases, like arthritis. Traumatic causes on the other hand, are due to any type of acute injury, most commonly seen in sport-related trauma. These injuries are mostly due to tensile overload, impingement and anterior glenohumeral instability (Blevins, 1997).

Extrinsic factors include impingement, tendonitis or tears due to influence from a defective coracoacromial arch, being either down-sloping, hooked or curved (Romeo *et al*., 1999; Seitz *et al*., 2011; Pandey *et al*., 2015) (Figure 2.3). Intrinsic factors include influences within the tendon, such as degeneration on a cellular level due to overuse, which might comprise of collagen thinning, proteoglycans, muscular dystrophy and vascularity changes, fatty degeneration to name a few (Lewis, 2009; Seitz *et al*., 2011; Pandey *et al*., 2015). Other factors that might influence RC tears and postoperative outcomes include; patients' age, lifestyle (smoking); body mass index (BMI); diseases or disorders (osteoporosis); and severity of the tear as examples (Wildemann and Klatte, 2012; Pandey *et al*., 2015).

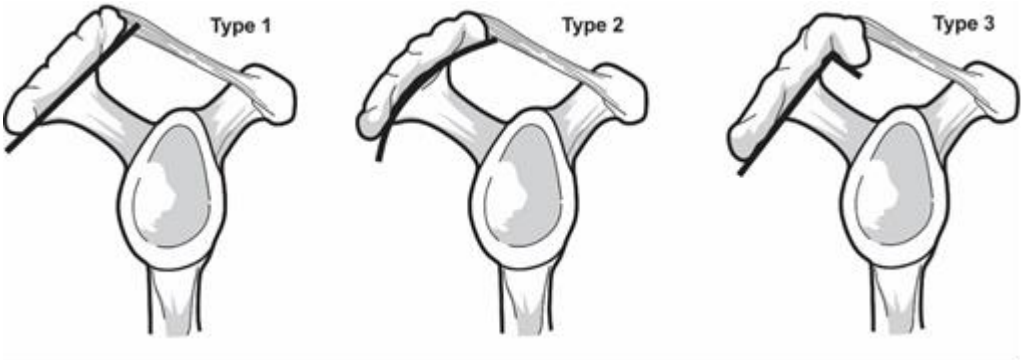

Figure 2.3 Types of coracoacromial arches

Although classifications have been made to explain pathoaetiology, it is known to be multifactorial. Therefore, surgeons must consider intrinsic, extrinsic and environmental factors when classifying the cause of RC tears (Lewis, 2009).

2.3.2 Classification of RC tears

One of the factors most commonly considered when classifying a tear, is its size, for example; small, medium, large or massive tears. Other factors, more recently considered, is the shape of the tear and tendons involved in the tear. Snyder's and Ellman's classification emphasizes the size of the tear and classifies it based on a grading system to determine the type of surgical treatment needed, for example using Ellman's classification, Grade 1 tear is <3 mm deep, Grade 2 is tear 3–6 mm deep and a Grade 3 tear >6 mm deep. Snyder's classification system is also used for full thickness or massive tears, due to its detailed grading system. Other classification systems used for full thickness/massive tear include DeOrio and Cofield classification systems, which looks at the anterior to posterior length of the tendon that is torn off of the humeral head (Belangero *et al*., 2013). According to the classification system of Cofield, the size of the tear is measured as follows, small < 1 cm; medium 1-3 cm; large 3-5 cm; massive > 5 cm.

Classification systems including the systems of Harryman and Gerber, looks at how many tendons are involved in the tear and is important to determine the type of surgery and

the degree of the procedure needed (Davidson *et al*., 2010; Belangero *et al.*, 2013). It is vital toconsider all the types of classifications, (which include different aspects) like shape, size, tissue involvement, is needed for the surgeon to make a decision on their approach. Treatment for small or partial thickness tears will frequently betreated using physical therapy, depending on the severity and position of the tear. However, these treatments do not necessarily repair the tear, but only improve function, pain tolerance and mobility of the shoulder. Tears that are classified as massive or full thickness tears on the other hand, will require surgical repair (Eisenberg, 2010). It is important to notice that there is not a single classification system that considers all these aspects in one and that is why a combined approach is advised (Belangero *et al.*, 2013).

2.3.3 Surgical approach for RC repair

Various surgical approaches are considered for RC tear repairs, namely arthroscopic, traditional open surgery and mini-open. Arthroscopy and mini-open approaches make use of suture anchors or anchors/transosseous combinations that are placed into the medial and lateral aspects of the greater tubercle to secure the torn tendon. These two methods are known, and popular, for their minimally invasive nature, reduced tissue retraction and lower postoperative complications (Ghodadra *et al*., 2009). However, numerous downfalls for these procedures have been reported, including high failure rates (up to 94%), decreased/limited movement and strength, postoperative pain, suture anchor malfunction and the cost of the procedure (Kim *et al*., 2006; Le *et al*., 2014; Ahmad *et al*., 2015). Suture/anchor malfunctions can be due to anchors pulling out of the bone, sutures tearing through tendons or creating new weak points allowing tears to occur in other places (Cummins and Murrell, 2003; Bishop *et al*., 2006; Kuroda *et al*., 2013).

Arthroscopic approaches also offer different suturing techniques during surgery, namely, single row, double row and transosseous equivalent repair. The transosseous approach requires drilling a tunnel/tunnels through the humeral tubercles to attach the torn tendon to the bone. The position of the repair is confirmed and an approximate tunnel of 2.4 mm is drilled into the greater tubercle, depending on the surgeon's preference. After this, the sutures are pulled through the tunnels using an all-suture implant and depending on the surgeon's approach, they might use anchors and sutures to secure tendon to bone or only sutures to fix the tendon to bone. (Aramberri-Gutiérrez *et al*., 2015; Black *et al*., 2015). This arthroscopic transosseous repair technique was introduced due to the downsides the anchors present, which includes migration of anchors, anchors pulling out of bone and allergic reactions towards anchors to name a few. The second reason for the popularity of this technique is, because several anchors are usually required for massive/large tears, but if bone quality is poor, anchors will not be the preferred option (Cummins and Murrell, 2003; Bishop *et al*., 2006; Kuroda *et al*., 2013).

The single-row anchor repair is performed by placing only one row of anchors just lateral to the articular margin of the humeral head. The anchors can then be single, double or

triple loaded with suture braids, which are subsequently passed through the tendon and the stiches secured (mattress stitch, half-hitch). The double-row anchor technique adds an additional two anchors along the lateral surface of the greater tubercle (footprint). Sutures are then passed through the tendon to the adjacent anchors and the tendon is secured to the humerus via a commonly used simple suture conformation (Kim *et al*., 2006; Franceschi *et al*., 2007). Results from recent studies tend to favour the double row anchor repair above single row, as it gives a seemingly better tendon-to-bone fixation and a larger footprint contact area, showing better biomechanical integrity compared to single row repair (Franceschi *et al*., 2007; Sugaya *et al*., 2007; Greenspoon *et al*., 2016; Hohmann *et al*., 2017).

The traditional open surgery, which is known as a more invasive approach makes use of a transosseous bone tunnel technique, using only sutures and the overlaying structures for the repair of the RC tear. The procedure includes retraction of the deltoid muscle and other overlaying tissue. This technique then allows surgeons to have a clear view of the complete RC unit and better accessibility to repair the tear without using anchors, which have been shown to pose a number of problems. A bone tunnel is drilled through the tubercle and sutures are then pulled through the tunnel by using suture techniques such as, the Mason-Allen suture technique to fix the tendon to the bone (Ghodadra *et al*., 2009). The transosseous procedure has shown to only produce re-tear rates of up to 6% according to Kuroda et al. (2013) and a success rate of between 80% and 94% according to Ghodadra *et al*., (2009). This method also generally yields better postoperative results, including improved movement, pain management and overall satisfaction (Ghodadra *et al*., 2009; Kuroda *et al*., 2013). Aside from the clinical benefits, open surgery using the transosseous technique is also more affordable than arthroscopic repair as it excludes the use of expensive anchors and the arthroscopic equipment.

Mini-open technique is merely a combination of the open and arthroscopic technique and makes use of suture anchors or transosseous equivalent technique. This technique uses arthroscopy to perform a subacromial decompression including the release of the coracoacromial ligament and subacromial bursal debridement. This technique avoids deltoid takedown, which involves splitting the deltoid without detaching the origin of the deltoid from the acromion, which makes it less invasive, yet more approachable (Kang *et al*., 2007; Ghodadra *et al*., 2009). The same approach is then used for implanting the arthroscopic anchors or the transosseous technique.

2.3.4 Postoperative complications of RC surgeries

Postoperative complications for RC surgery are addressed across several resources such as research publications, internet sites and pamphlets, yet some of the major comlications are sometimes not discussed thoroughly during RC surgeries. The most important step to overcome and prevent these complications is to thoroughly consider all options pre-operatively, as well as postoperatively with the knowledge of each complication (Randelli *et al*., 2011; Thakkar *et al*., 2014). Techniques used to detect postoperative

complications include CT and MRA scans of the patient's shoulder with special focus on the RC unit.

The most common and broadly discussed complication is re-tear of the fixed tendon, which often presents with pain and decreased function of the shoulder after surgery. Re-tears can be due to extrinsic or intrinsic factors, or factors that include suture failure, anchor pullout/displacement and subacromial spurs or incorrect physical therapy. (Millstein and Snyder, 2003; Kim *et al*., 2008; Randelli *et al*., 2011; Thakkar *et al*., 2014). Re-tear from poor healing can be attributed to patient age and associated age-related disorders namely, osteopenia, osteoporosis, poor tissue quality etc. Other factors that may contribute to the re-tear of the tendon includes, size of the tear, lack or reduction of vascularization around the tear and footprint area, fatty infiltration and atrophy/retraction of the cuff muscles (Randelli *et al*., 2011; Mall *et al*., 2014; Kokmeyer *et al*., 2016).

Humeral head necrosis or otherwise known as osteonecrosis is another complication that involves bone loss or death of bone (Mayoclinic.org, 2016) (Figure 2.4). This is specifically related to the use of suture anchors during arthroscopic RC repair (Dilisio *et al*., 2013; Goto *et al*., 2013; Parada *et al.*, 2014). The exact aetiology is currently still unknown and under debate. However, some research has suggested that this condition may arise due to the insertion of multiple anchors or abnormal anchor placement, which may obstruct and potentially damage the direct vascular supply of the RC leading to stiffness, poor healing, infection, deep venous thrombosis, cyst formation and soft-tissue inflammation (Dilisio *et al*., 2013; Goto *et al*., 2013; Thakkar *et al*., 2014) (Figure 2.5). Another condition that has been directly linked to the arthroscopic approach is postarthroscopic humeral chondrolysis (PHC). PHC is a severe type of shoulder arthritis in which the joint cartilage disintegrates rapidly as a result of lysis of the chondral matrix or dissolution of the cartilage matrix and cells (Bailie and Ellenbecker, 2009). The actual cause of reported cases has not been confirmed, but may be linked to the following: thermal probes, pain pumps, intra-articular local anesthetic and suture anchor placement, which are known to be associated with arthroscopic surgery. (Yeh and Kharrazi, 2012; Parada *et al.*, 2014).

Figure 2.4 Humeral head necrosis or otherwise known as osteonecrosis (Habermeyer, Magosch and Lichtenberg, 2006)

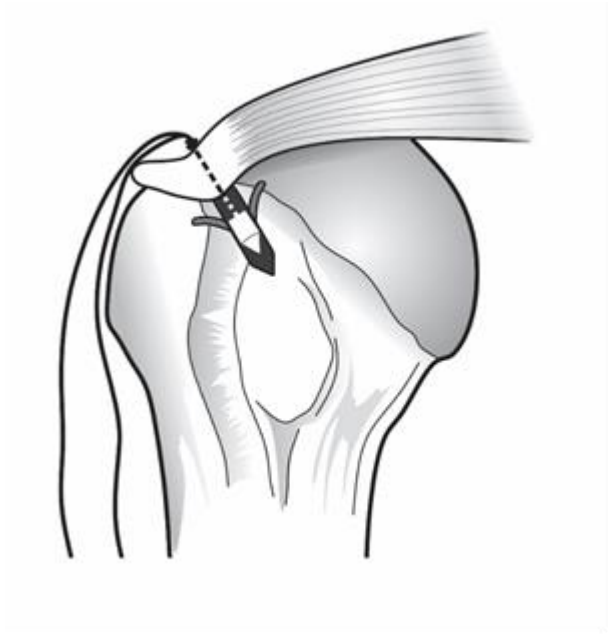

Figure 2.5 Anchor placement in the bone-cartilage junction (Burkhead et al., 2007)

Postoperative function of the RC is another factor still under debate, however, in most cases, open surgery using transosseous techniques has shown favour, presenting good to excellent outcomes with regard to functional improvement (75–95 % of patients) and pain relief (85–100 %) (Ghodadra *et al*., 2009; Seida *et al*., 2010). It is also seen as the most successful technique for large to massive rotator cuff tears with a high rate of RC integrity

(Klepps *et al*., 2004; Ghodadra *et al*., 2009; Aleem and Brophy, 2012). Arthroscopic techniques using suture anchors, despite showing favourable outcomes as well, tend to lower or alter the biomechanical strength and compromise the integrity of the GHJ and RC complex after repair, which is concerning. This has led to inconsistent results regarding functional improvement, specifically over a long period, with most cases resulting in a re-tear rate between 11% and 94% (Liu and Baker, 1994; Klepps *et al*., 2004; Le *et al*., 2014).

2.4. Biomechanics of the RC

2.4.1 Surgical tensile technique testing

Several biomechanical studies have been performed to evaluate the efficacy of different types of surgical techniques and surgical material used for RC repair on both fresh and cadaveric specimens. The methods used in these studies differ slightly from study to study but in general, when testing a repair technique, a soft tissue clamp is used to secure the proximal end of the RC tendon to a testing machine and the humerus is tightly secured in some sort of jig to stabilize it. These testing devices are known as materials testing machines/systems (MTS), with the most common one being the Instron 8872 servo-hydraulic testing instrument. The tendon is prepared for the tensile testing, for example, mounting the tendon in a standard orientation, applying the correct load for the test, placing the laser reflection system on the area where tension is to be recorded; simply using a cyclic load to failure test or a single load to failure test to evaluate tension (Kim *et al*., 2006; Weber *et al*., 2015).

The techniques that utilize suture anchors, and especially double row techniques, seem to produce better outcomes during these tensile strength tests, with a mean number of cycles to failure of 1414 after 5000 cycles, whereas the transosseous bone tunnel technique have shown weaker results with a mean number of cycles to failure of only 528 after 5000 cycles (Waltrip *et al*., 2003; Hohmann *et al*., 2017). These results contradict the fact that patients who have had transosseous repair yielded a much higher success rate, with 80-94% overall in comparison with the failure rate of up to 94% of suture anchor techniques. (Klepps *et al*., 2004; Ghodadra *et al*., 2009; Behrens *et al*., 2011; Le *et al*., 2014). The problem that these tests present is that they do not include natural movement or strain on the tendon or overlaying tissue repair, which are just some of the critical steps that form part of the integrity and success of these techniques. Due to these factors being avoided, the integrity of the results has raised suspicion. Additionally, the biomechanical test studies often do not follow a golden standard of testing etiquette and often these tests make use of different materials, different shoulder angles, different stitching techniques, different pre-loading conditions (Hohmann *et al*., 2017). This, and the above mentioned exclusions, should make the results of these studies interpreted with caution.

2.4.2 Tendon testing

Other biomechanical studies, not necessarily focused on surgical techniques, include determining the tensile strength of standalone tendons, and also how much strain and stress these tendons can bear before they tear. These studies involved harvesting strips of the rotator cuff tendons, testing them individually or, in some cases using the complete RC unit and testing the tensile strength by means of a cyclic loading system (Itoi *et al*., 1995; Weber *et al*., 2015). In these cases, the tendons are intact, meaning still either attached to the humeral tubercles, or loose from the tubercles.

The steps to perform these tests are similar to testing the surgical techniques, except only the harvested tendon (pure tendon) is tested. Another test can also be performed to determine the fibre properties of each layer that consists of the unit. These tests are performed using markings known as beads with laser beam sensors to detect displacement in fibres while undergoing the tensile test (Huang *et al*., 2005; Lake *et al*., 2009). A study done by Huang et al. (2005), tested the supraspinatus tendon tensile strength, by pulling the tendon in different directions. This test involved fixating the humeral shaft in a custom built clamp and the tendon part held by a grip. The markers were then placed in a specific order to represent the different areas of the tendon. A total mean value for load and standard deviation were one of the measurements obtained and were 1007.1±426.1 N and a total stress value of 11.5±5.0 MPa were also measured. Another study done by Itoi *et al*. (1995) tested cadaveric specimens and used the supraspinatus anterior strips, which yielded an ultimate load of 411.1 N and a posterior strip which yielded a load of 88 N. The most referred to study used in this case was a study done by Nakajima et al. (1994), where the specimens were separated into the 2 layers (bursal/tendinous and capsular) and tested with insertion still attached to humeral tubercles. This study also used test to failure as one of their methods and showed a difference in the 2 layers. The bursal/tendinous layer was twice as strong as the capsular layer when comparing ultimate failure and the overall Newton force displayed by the supraspinatus (SS) was an eighth of the amount compared to previous studies which yielded 454 kg tensile load. Once again bead markers were used and placed on specific locations on the tendons and tested using a slightly different clamping method, by clamping the tendon between 2 clamps and pulling until failure. In this study, the focus was on stress value, measured in MPa, using the median values which included numerous position results, but to give a few: the anterior bursal (0.19 MPa); posterior bursal (0.12 MPa); anterior joint (0.18 MPa); posterior joint (0.08 MPa). This study concluded that different fibres in different locations of the RC tendons were in fact different when looking at stress strain alone.

These findings should be considered during RC repairs, as mentioned it is said that the RC unit is made up of different layers consisting of different fibre properties (Clark *et al*., 1992; Nakajima *et al*., 1994). This alone should raise interest when repairing a torn tendon, as it is not only the tendon that needs to be repaired, but also the complete unit with the other layers that this RC unit comprises.

One of the most important layers as mentioned is the IC/capsular layer, which consists mainly of a sheet of interwoven collagen fibres that interdigitate with the tendons proximal to their insertion point onto the tubercles (Clark *et al*., 1992; Vosloo *et al*., 2015). According to Nakajima et al. (1994) the IC/capsular layer and the overlaying tendon (bursal/tendinous layer) layer clearly reveal a difference in biomechanical properties (De Beer, *per comm;* Clark *et al*., 1992; Adam *et al*., 2016). According to their results, the supraspinatus (SS) bursal/tendinous layer yielded twice the ultimate failure stress than the capsular/joint layer. This is due not only to the fibre direction of these layers, but also due to the fibre properties in these layers, resulting in different load strength across the RC unit. Nakajima et al. (1994) found that the overlaying tendinous layer consisted mainly out of longitudinal fibers, which are thicker and more elastic, resulting in a higher load stress. Whereas the IC or joint capsule comprised mainly out of lengthwise and crosswise interconnected fibres which were thinner than the tendinous layer, making it less elastic, resulting in lower stress load and earlier failure. According to Nimura et al., (2012), degenerative tears can originate from posterior due to the IC being so thin and evidently result in a tendinous tear. This is one of the factors currently most overlooked by surgeons, as repair is only focused on the overlaying tendinous layer, ignoring the joint capsular layer; this needs to be repaired according to its fibre properties. Repairing the overlaying tendinous layer, disregarding the IC layer only provides a temporary fix and usually results in a full thickness re-tear (De Beer, *per comm;* Nimura *et al.*, 2012,.

Chapter 3: Materials and methods

This study used a quantitative, experimental approach to investigate the biomechanical properties of the capsular and tendinous layers of the RC tendons. This approach included testing the tensile strength of the supraspinatus (SS), infraspinatus (IS) and subscapularis (SC) tendinous and capsular layers. The current study was designed to evaluate the biomechanical properties of healthy RC tendons in a South African population.

3.1 Materials

The total sample was comprised of 17 fresh/frozen shoulder specimens and 5 cadaveric shoulders. Of the fresh shoulders 13 were harvested from 9 white males (right = 7; left = 6) and 4 were harvested from 2 white females (right = 2; left = 2). The age of the total fresh sample ranged between 54 and 83 years of age (mean = 64.6 years). Of the cadaveric shoulders, 2 were harvested from 1 male cadaver (right = 1; left = 1) and 3 were harvested from 2 female cadavers (right = 2; left = 1) and the cadaveric age ranged between 34 and 82 years of age (mean = 64.7 years). The fresh shoulders were obtained from the National Tissue Bank under the auspices of the University of Pretoria with ethical clearance from the Faculty of Health Sciences Research Ethics Committee (239/2015). The cadaveric shoulders were obtained from medical dissection halls in the Department of Anatomy, University of Pretoria. These cadavers are received from donations to the Medical faculty for the purpose of teaching and research.

Only adult shoulders (>25 years), without any known injury, pathology or previous shoulder surgeries were included**.** Sex, weight, height and population affinity was not considered an exclusion factor and were recorded for all samples. Degeneration of tendons do occur with age, but due to the wide range of results, with no correlation to age, it was not seen as an inclution factor. The only factor that might have had an effect was the personal fitness and wellbeing of each patients, but could not be determined. Studies have previously shown that the chemicals utilised during the embalming process have a significant effect on the biomechanical properties of the muscles and tendons (Wilke *et al*., 1996; Verstraete *et al*., 2014), therefore this study included embalmed specimens as a comparison base for the fresh shoulders. Not all institutes, both National and International, make use of the same embalming procedures and chemicals, therefore this study analysed the effect of the procedure utilised in the Department of Anatomy at the University of Pretoria.

3.2 Methods for tendon testing

The cadaveric and fresh specimens were dissected and prepared one month before the testing took place. The cadaveric specimens were stored in a container with embalming fluid and kept in a cool dry place. The fresh specimens were frozen (-5^{o}C) and stored in labelled containers in a walk-in freezer in the Department of Anatomy. Although several studies have demonstrated that freezing can affect the biomechanical properties of soft tissues

(Venkatasubramanian *et al.,* 2006; Chow and Zhang, 2011), there are still contradictions in this regard as several papers have stated that no alterations in the physical and histological properties could be noted (Panjabi *et al.,* 1985; Bitar 2010). The method used to correctly and carefully dissect out the RC tendons and joint capsule is detailed below.

3.2.1 Tendon harvesting method

The RC unit of each specimen was exposed by removing the skin, subcutaneous tissue, fat and the deltoid muscle using standard dissection methods and equipment. This enabled a clear visualization of the RC unit. Thereafter, a reverse dissection was done, removing the RC muscles from their scapular origins towards their insertions onto the humerus. In order to remove the complete RC unit from the scapula, the joint capsule at the glenoid labrum was cut as close as possible to its attachment to the glenoid fossa and the coracohumeral and coracoacromial ligaments were sectioned. This resulted in a specimen only comprising of the tendinous and capsular parts of the RC unit attached to the humerus together with a small section of the reflected RC muscles from their scapular origins. The RC unit was then removed from its humeral attachment by a systematic approach, cutting as close as possible to the humeral insertional zones to minimize damage to both capsular and tendinous layers.

Once the RC unit was completely detached from both the scapular and humeral attachments, they were either stored in embalming fluid (cadaver specimens) or frozen (fresh specimens) in labelled containers.

3.2.2 Tendon testing method

The fresh specimens were thawed 24 hours before testing to return them to their natural state. The tendons of the RC unit (subscapularis, supraspinatus and infraspinatus), including the areas of known interdigitation, were then cut into longitudinal strips of 40 mm in length and 25 mm in width (Figure 3.1). The bursal/tendinous (outer) layer was then separated from the capsular layer (inner) as far as possible. These strips comprised only out of tendon (no muscle) with intact, non-separated, superficial bursal (outer).

Figure 3.1 Strip of SS bursal layer (external view)

The tensile tests were performed using a benchtop MTS Criterion Model 41 tensile testing machine for composite materials, loaded with a 1kN load cell (Figure 3.2).

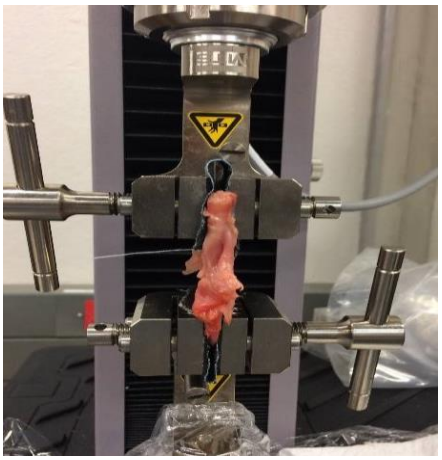

Figure 3.2 MTS Criterion Model 41 with tendon specimen secured by clamps

The tendons were secured with rubber soft tissue clamps and reinforced with sand paper to ensure minimal slippage and pressure at the ends of the RC strip (Figure 3.2).

The strips were kept moist with a standard phosphate buffer solution (PBS) during the whole process. Each strip was tested individually to failure at a constant rate of 0.5 mm/s and the results were recorded using the MTS Test suit TWE 4.1.5.736, showing the maximum Newton force reached at failure point. The measurements required for this study included: the peak load (maximum force) of each layer within the different tendons, measured in Newton force (N) and the modulus of elasticity, measured in megapascals (MPa). The tensile strength is defined as the resistance of the tendon to breaking under tension (pulling of the tendon) and the modulus is the ratio of stress to correspond to strain in the tendon under tension (Kent, 2017). For this sample in the study, the peak load was taken as the maximum tensile strength

and was recorded before the first tears occurred and decreased in tensile strength in the tendon samples. There was slight slippage of the tendons in the clamps that occurred during the test, but the peak load was still able to be taken.

For the capsular layer, the same approach was used to remove the complete RC unit from the humeral head. The capsular and bursal/tendinous layer were then separated as far as possible towards their insertion onto the humerus. The two layers were not forcefully separated from one another, but remained intact at the RC insertion area (Insertion onto bone), this being done to retain the integrity of the results. The intact area was placed in the soft tissue clamp and reinforced with sand paper. The same was done for the opposite end, which consisted only out of the capsular layer and was then also reinforced with sand paper to prevent slippage. The strips were also tested individually until failure at a constant rate of 0.5 mm/s, using the MTS Criterion Model 41, Benchtop tensile testing machine and results were recorded on MTS Test suit TWE 4.1.5.736., showing the maximum Newton force at failure point.

3.3 Statistical analysis

For the statistical analysis, the samples were categorized as follows: cadaveric sections (SS, IS, SC), fresh bursal/tendinous sections (SS, IS, SC) and fresh capsular sections (SS, IS, SC). All statistical analyses were done using IBM SPSS statistical package Version 21. All the peak load (N) and modulus (MPa) data were firstly analysed to obtain descriptive statistics, which included establishing the mean, median, minimum and maximum value, as well as the standard deviation, providing a comprehensive overview of each data set. For each data set, a box plot was constructed to provide further insight into the distribution of the data and to observe any outliers. Box plots display the five number summary of a data set including the minimum and maximum, the median as well as the first and third quartile (Khan Academy, 2018). Box plots also provide a visual representation to observe if the data is symmetrical, how tightly the data are grouped and also, to see if the data are skewed and in what direction (Datavizcatalogue.com, 2018)

Determining the distribution of a data set is an important step for parametric tests as the validity of these tests are dependent on the normality of the distribution (Ghasemi and Zahediasl, 2012). A Shapiro-Wilk test for normality was used to establish whether the data were normally distributed or not normally distributed. Shapiro-Wilk was selected as it is the appropriate test for smaller sample sizes (https://statistics.laerd.com/spss-tutorials/testing-for-normality-using-spss-statistics.php). The basis of the Shapiro-Wilk test is that the hypothesis of normality is rejected if the p-values is less than or equal to 0.05 (http://www.variation.com/da/help/hs141.htm). If the p-value is less than or equal to 0.05 then it can be stated with 95% confidence that the data are not normally distributed and if the p-value is greater than 0.05 then it can be stated with 95% confidence that the data are normally distributed.

Comparative statistical analyses were used on the normal and nonparametric data sets to determine whether the different layers and tendons differed significantly from each other with regard to load to failure (N) and elasticity (modulus – MPa). The normally distributed data were analysed using a two sample t-test to determine whether two population means are equal or not. The two sample t-test is a common test used to determine whether average differences between two groups is really significant or rather due to random chance instead (https://www.isixsigma.com/tools-templates/hypothesis-testing/making-sense-two-sample-t-test/). The data that were not normally distributed, p-values less than or equal to 0.05, the nonparametric Mann-Whitney u test (test for equal medians) was used to compare the sample means to see if they were equal or not. This test is an appropriate alternative to the independent sample t-test (http://www.statisticssolutions.com/mann-whitney-u-test/) when no inference is made or attributed to data distribution.

Chapter 4: Results

The biomechanical results were generated through the MTS Test suit TWE 4.1.5.736., which is used to analyse and process the results from the MTS Criterion Model 41 as the testing was done. All the results were then prepared for the different statistical analyses to be done. These analyses included descriptive statistics to establish the means, medians, standard errors and standard deviations of the different samples. Box plots were also constructed to visualise the data dispersion around the mean. Graphical representation of the tendon testing was automatically generated through the MTS program. The graphs showed the peak load in Newton force over the extension in millimetres and on a separate section in the program it also calculated the modulus in MPa. The modulus can be seen on the graphs and provides information as to the elasticity of the tendons under the testing conditions, but for better interpretation, the results for the modulus is seen more as the flexibility, instead of the elasticity of the tendon. Following normality tests of the data, comparative statistics were also run to determine if a significant difference exists in the biomechanical properties between the bursal/tendinous (outer) and capsular (inner) layers of each of the RC tendons and areas of known interdigitation as well as to determine the differences between the biomechanical properties of the fresh shoulders versus the cadaveric (embalmed) shoulders.

4.1 Descriptive statistics for cadaveric and fresh tissue samples

4.1.1 Summary statistics: Peak load (N) and Modulus (MPa) for individual tendons

Descriptive statistics: Peak load

The highest average peak load for all three tendons, supraspinatus (SS), infraspinatus (IS) and subscapularis (SC) in the entire sample, was seen in the cadaver specimens with averages of 548.2±116.8 N (SS), 432.6±106.1 N (IS) and 452.0±97.2 N (SC) (Tables 4.1,4.2 and 4.3). With regard to just the fresh samples, the highest average peak load values for the individual tendons were observed in the capsular layers of supraspinatus (232.0±52.4 N)(Table 4.1) and infraspinatus (IS) (203.9±39.4 N)(Table 4.2) and in the bursal layer for subscapularis (SC) (254.6±52.5 N)(Table 4.3). The lowest average peak load values in fresh samples for the individual tendons were seen in the bursal layers of supraspinatus (SS) 190.1±39.0 N (Table 4.1) and infraspinatus (IS) 171.1±19.9 N (Table 4.2) and in the capsular layer of subscapularis (244.9± 95.7 N) (Table 4.3).

Table 4.1 Summary statistics for the peak load values for Supraspinatus (SS) measured in Newtons (N)

	Cadaver SS	Bursal SS	Capsular SS
N	5	12	4
Min	183.5	11.6	153.6
Max	811.5	446.8	426.8
Mean	548.2	190.1	232.0
Std. error	116.8	39.0	65.4
Stand. dev	261.2	135.1	130.8
Median	552.7	209.3	173.8

Table 4.2 Summary statistics for the peak load values for Infraspinatus (IS) measured in Newtons (N)

	Cadaver IS	Bursal IS	Capsular IS
N	5	12	4
Min	89.7	74.2	108.2
Max	694.0	254.3	271.9
Mean	432.6	171.3	203.9
Std. error	106.1	19.9	39.4
Stand. dev	237.3	69.1	79.2
Median	468.9	182.7	217.9

Table 4.3 Summary statistics for the peak load values for Subscapularis (SC) measured in Newtons (N)

	Cadaver SC	Bursal SC	Capsular SC
N	4	11	5
Min	218.7	45.7	32.0
Max	691.9	548.9	558.3
Mean	452.0	254.6	244.9
Std. error	97.2	52.5	95.7
Stand. dev	194.5	174.0	213.9
Median	448.8	229.6	168.6

In Figure 4.1, both the cadaver and the bursal SS layer display a wide range of load to failure compared to the capsular SS layer, which displays a much narrower range. Although a large load to failure range is seen in cadaver SS layer, the data is somewhat equally dispersed around the median. Both the bursal and capsular SS layers showed skewed dispersion with the bursal SS being skewed toward the lower limit of the box plot and the capsular towards the upper limit of the box plot. It is also clear from Figure 4.1 that the capsular SS layer is not equally dispersed as the data is skewed with the box positioned towards the bottom whisker with a limited data distribution overall and the median value also towards the bottom whisker. The median values for the capsular and bursal SS layers are similar to each other but

a clear difference can be observed between these two layers and the cadaver SS median, which is much larger (Figure 4.1).

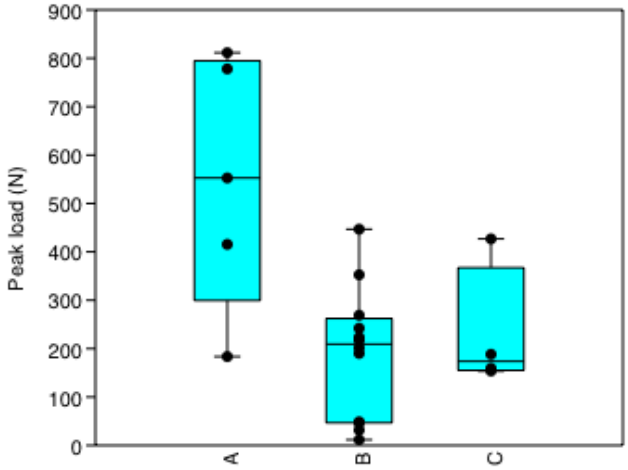

Figure 4.1 Box plot for supraspinatus peak load (N) values (A – cadaver SS; B – bursal SS; C – capsular SS)

For Figure 4.2, the cadaver IS layer display a wide range of load to failure compared to both bursal and capsular IS layers, which displays a much narrower range. The same, somewhat equal data distribution can be seen around the median as with the cadaver SS layer. For the bursal and capsular IS layers, the IS data is more equally dispersed around the median with no outliers and a well distributed box between top and bottom whisker. The median values for the capsular and bursal IS layers are similar to each other, but as with the SS layer, a clear difference can be observed between these two layers and the cadaver IS median, which is much larger (Figure 4.2).

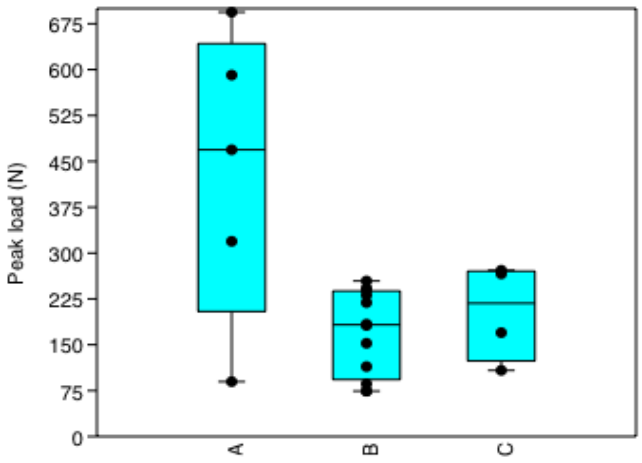

Figure 4.2 Box plot for infraspinatus peak load (N) values (A – cadaver IS; B – bursal IS; C – capsular IS)

Figure 4.3 also shows a well distributed cadaver SC layer, as well as a bursal and capsular SC layer. Both bursal and capsular SC layers, displays a much wider range of load to failure, coming into closer range of the cadaver data distribution. The bursal SC layer displays a wide range of failure compared to the SS and IS layers (Figure 4.1 and Figure 4.2), although still normally distributed, skewed towards the lower limit of the bottom whisker. The capsular SC, although normally distributed, has a median skewed more to the bottom whisker of the data and also has a wide range displayed in Figure 4.3. The median values for the capsular and bursal SC layers are similar to each other, but as with the previous layers (Figure 4.1; Figure 4.2), a clear difference can be observed between these two layers and the cadaver SC median, which is much larger (Figure 4.3).

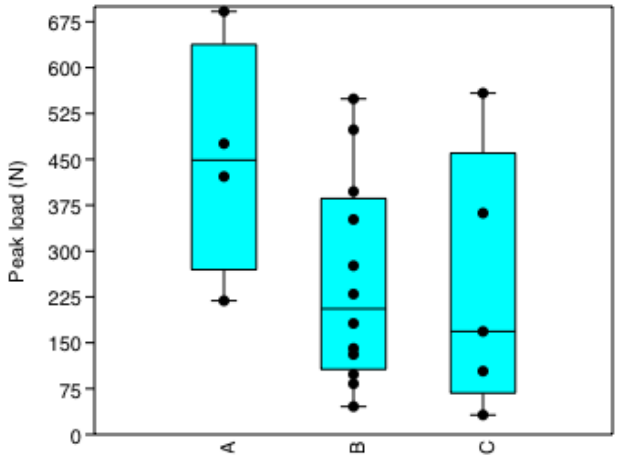

Figure 4.3 Box plot for subscapularis peak load (N) values (A – cadaver SC; B – bursal SC; C – capsular SC)

Descriptive statistics: Modulus

To measure the modulus, the cross-sectional area had to be known, which was roughly measured at time of testing with a ruler. It was then entered into the program which used the cross sectional area together with newton force to calculate the modulus (MPa).

The highest average modulus when looking at the fresh samples for supraspinatus (SS), infraspinatus (IS) and subscapularis (SC), was seen in the capsular SS layer with averages of 27,4±5.9 MPa (Table 4.4), in the cadaver specimens IS with an average of 47,2±26.3 MPa (Table 4.5) and bursal layer SC with average of 79,3±41.0 MPa (Table 4.6). The lowest average modulus values were observed for the cadaver SS layer with an average of 1.5±5.1 MPa (Table 4.4), the bursal IS layer with an average of 11.5±3.7 MPa (Table 4.5) and the capsular SC layer with an average of 0.9±7.5 MPa (Table 4.6).

Table 4.4 Summary statistics for the modulus (MPa) values for Supraspinatus (SS) measured in Newtons (N)

	Cadaver SS	Bursal SS	Capsular SS
N	3	5	4
Min	15.2	4.8	16.9
Max	43.3	22.9	44.4
Mean	1.5	15.5	27.4
Std. error	5.1	3.5	5.9
Stand. Dev	11.4	7.8	11.8
Median	31.2	19.0	24.2

Table 4.5 Summary statistics for the modulus (MPa) values for Infraspinatus (IS) measured in Newtons (N)

	Cadaver IS	Bursal IS	Capsular IS
N	3	5	4
Min	14.5	3.4	10.4
Max	99.2	24.8	48.5
Mean	47.2	11.5	23.5
Std. error	26.3	3.7	8.5
Stand. Dev	45.5	8.2	17.0
Median	28.1	11.2	17.5

Table 4.6 Summary statistics for the modulus (MPa) values for Subscapularis (SC) measured in Newtons (N)

	Cadaver SC	Bursal SC	Capsular SC
N	4	4	5
Min	11.0	36.7	3.5
Max	48.6	202.4	47.1
Mean	22.9	79.3	0.9
Std. error	8.7	41.0	7.5
Stand. Dev	17.3	82.1	16.8
Median	16.1	39.1	16.2

In Figure 4.4, both the cadaver and the capsular SS layer display larger modulus of elasticity values compared to the bursal SS layer. All three sections have well dispersed data with no major outliers. A larger modulus range is seen in cadaver SS layer, with the data equally dispersed around the median, despite having the box positioned more towards the upper whisker. Both the bursal and capsular SS layers showed skewed dispersion with the bursal SS being skewed toward the lower limit of the box plot and the capsular towards the upper limit of the box plot. The median values for the capsular layer lies more towards the upper limit of the box, whereas the median for the bursal SS layers are observed closer to the lower limit of the box.

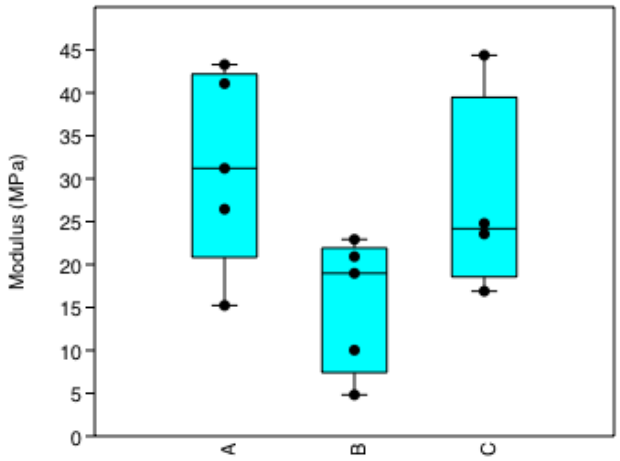

Figure 4.4 Box plot for supraspinatus modulus (MPa) values (A – cadaver SS; B – bursal SS; C – capsular SS)

A very wide range can be seen for the cadaver IS layer in Figure 4.5, with no whiskers displayed and a median value migrating towards the lower limit of the box. It also has the highest value for modulus, which is far above the modulus values for the capsular and bursal IS layer. The bursal IS layer has a very narrow range of modulus compared to the capsular SS layer, but still displays a normal distribution. Although a very narrow range, the bursal IS layer has a median value positioned closer to the middle of the box, with the box skewed towards the bottom whisker. The capsular IS layer has a box skewed towards the bottom whisker and median value positioned more towards the lower limit of the box. Even though these three layers display different data ranges, their median values are somewhat close to one another, taking the data range in consideration.

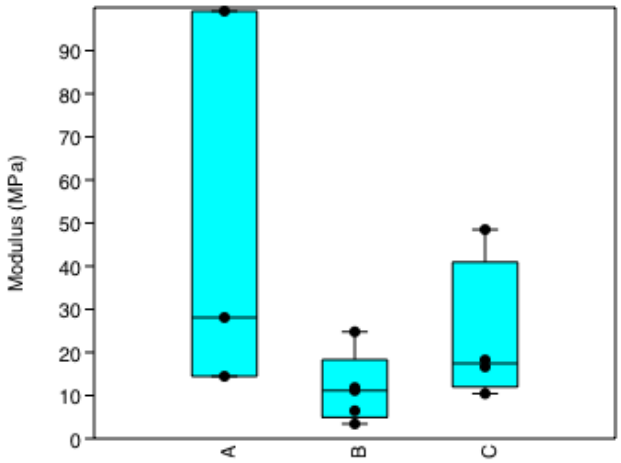

Figure 4.5 Box plot for infraspinatus modulus (MPa) values (A – cadaver IS; B – bursal IS; C – capsular IS)

In Figure 4.6, both the cadaver and the capsular SC layer display a very narrow range of modulus compared to the bursal SC layer, which displays a much wider range. Although a large modulus range is seen in the bursal SC layer, the data is not equally dispensed and the median is found at the bottom limit of the box, just as the box is also skewed to the bottom whisker. The data for the cadaver SC and capsular SC layer is narrow, but somewhat equally dispersed. Although the median for the cadaver SC is more to the lower limit of the box and the box is skewed towards the bottom whisker, the data is still normally distributed. The capsular data is also leaning more towards the bottom whisker, but with a median more towards the middle of the box. It is also observed that the median value for cadaver SC and capsular SC is very close to one another.

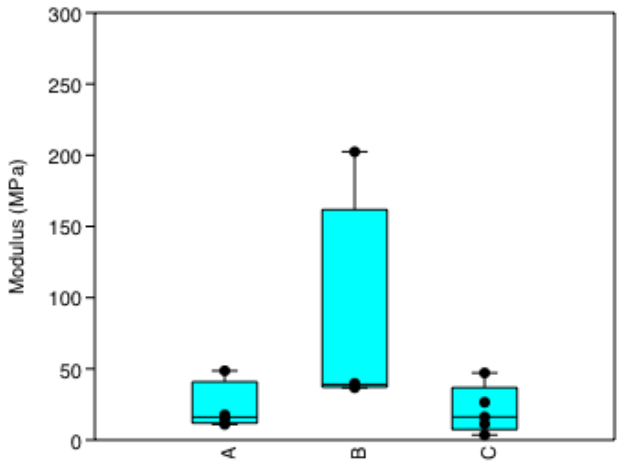

Figure 4.6 Box plot for subscapularis modulus (MPa) values (A – cadaver SC; B – bursal SC; C – capsular SC)

4.2 Graphical representation of load versus extension for cadaver and fresh sample specimens

In Figures 4.7 and 4.8, graphs for cadaveric specimens are shown (SS and IS). These graphs display a load versus extension curve; as the load is applied, reaching the yield strength (Figure 4.7 first circle) point where the graph starts to slow down and curve as deformation of the specimen takes place. As force is continually applied, the deformation section leads to the peak load (first diamond shape), which is the maximum force/tensile strength of the specimen. In these cadaveric specimens it is evident that the specimen can return slightly to original position (the increase and decrease "spikes/curves"), due to molecular make-up of the fibres, but then depicts a downward slope and eventually breakdowns (fracture) or weakens. There is not much "spiking" of the fibres in the cadaveric specimens, due to fibre bonds not functioning individually anymore, but rather functioning together, which can be due to an influence from the embalming process.

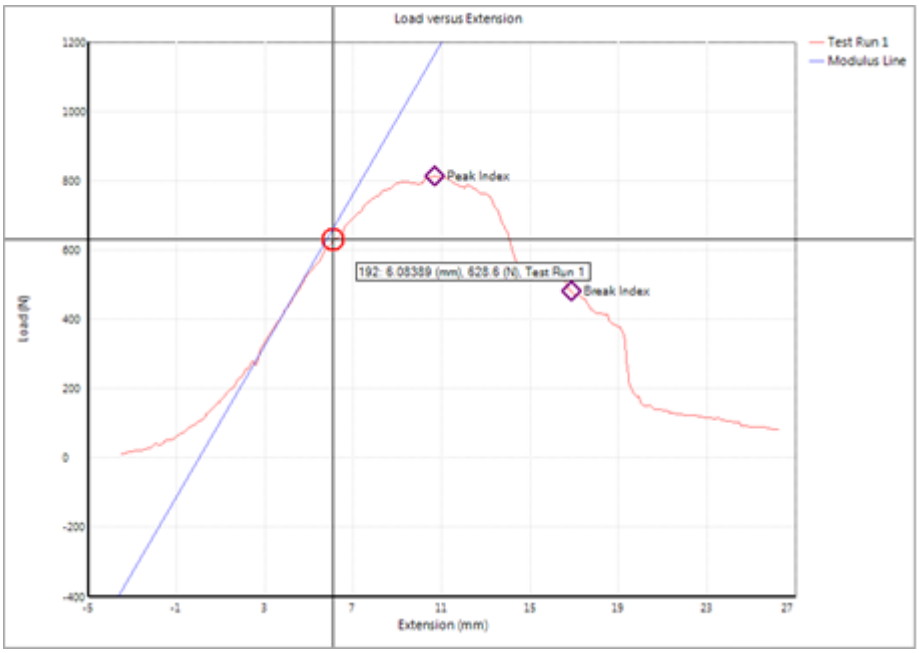

Figure 4.7 Load (N) versus extension (mm) graph for cadaver specimen SS (Right) depicting peak load (811.51 N) and modulus (31,21 MPa)

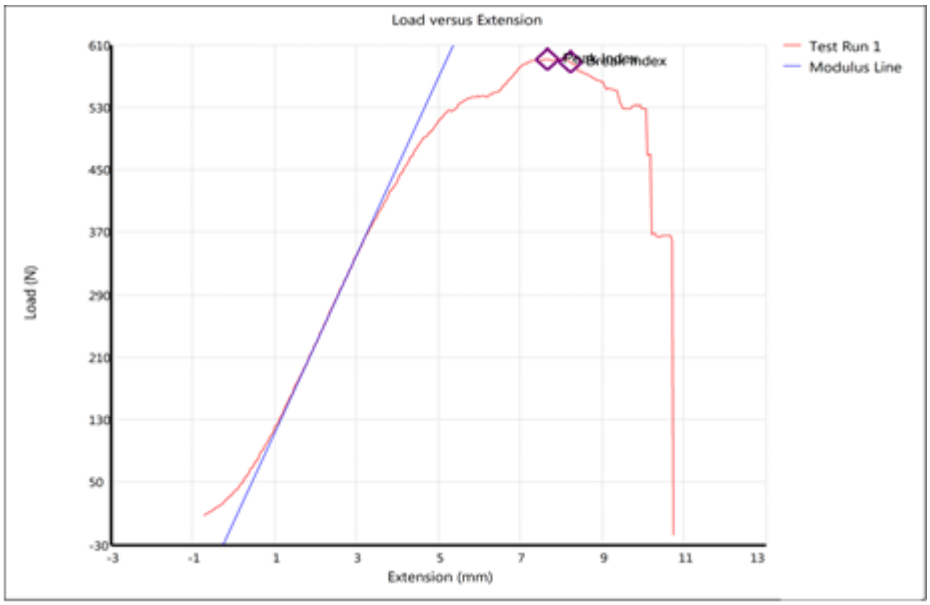

Figure 4.8 Load (N) versus extension (mm) graph for cadaveric specimen IS (Left), depicting peak load (591,087 N) and modulus (99,165 MPa)

Figures 4.9 and 4.10, graphs illustrate the peak load (N) and modulus (MPa) for the bursal/tendinous specimens for SS and SC layers. The overall image of these graphs are slightly different than that of the cadaveric specimens, as these bursal/tendinous layers

presents fresh tissue. The overall shape of the graph presents a sharper and higher centre, with longer tails at the bottom. In Figure 4.9, the bursal/tendinous layer displays deformation at the start, as force is applied, and at a certain point in the middle of the increasing strain, the first "spike" is seen, small as it curves and continues to increase, which presents the fibres functioning more independently. The load/extension gradient then increases as deformation takes place, but does not present a clear yield strength, rather continues to increase as it reaches the peak load. The same can be seen for Figure 4.10, with a much more even increase load/extension gradient, reaching peak load. As these bursal/tendinous layers deforms in the downward slope, the effect of individual fibre strength is presented clearly with clear "spikes". This is what makes it slightly different from the cadaveric specimens as well, is that the flexibility of the fibres are still unaffected by chemical processes and represents a more realistic and reliable outcome.

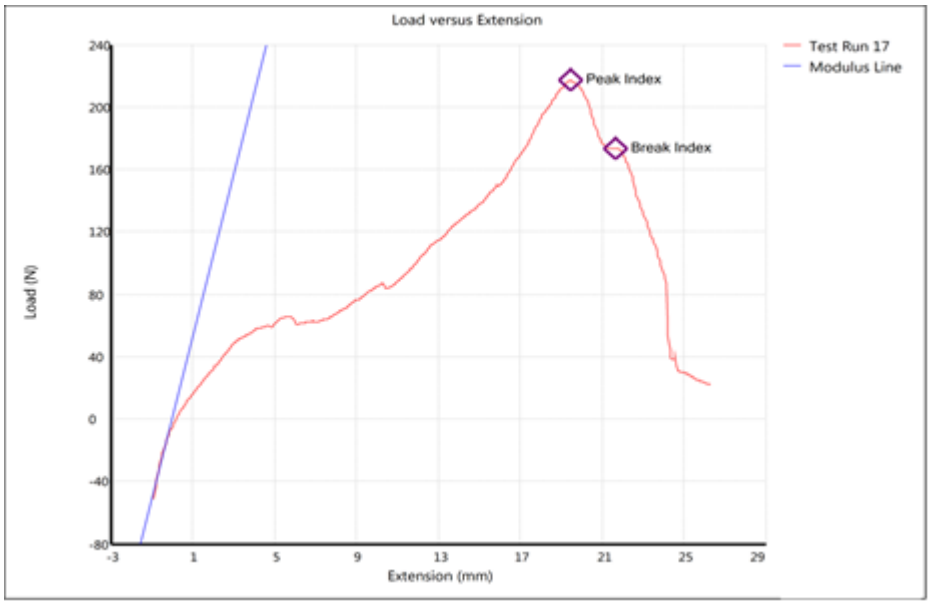

Figure 4.9 Load (N) versus extension (mm) graph for bursal specimen 7 (Left), depicting peak load (216,897 N) and modulus (20,921 MPa)

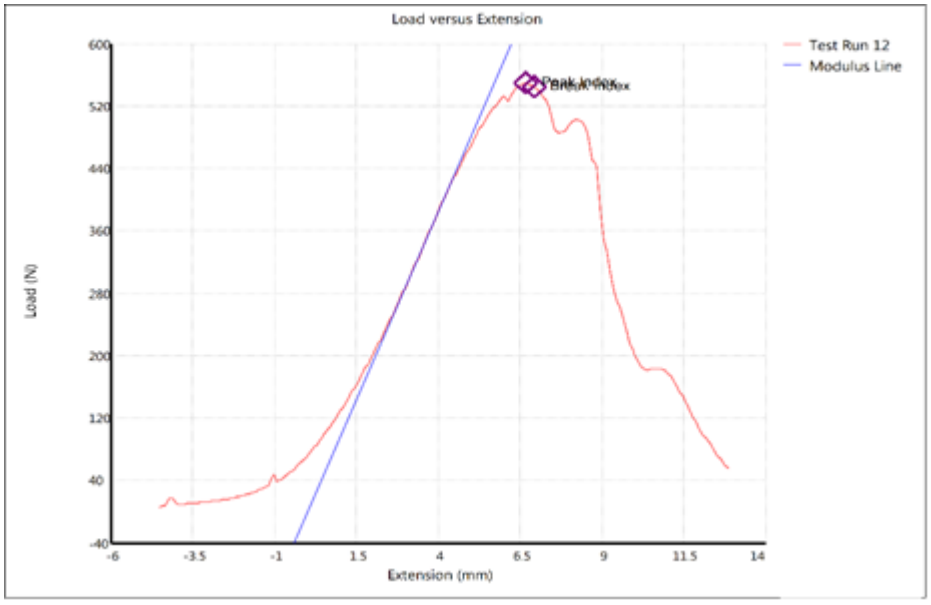

Figure 4.10 Load (N) versus extension (mm) graph for bursal specimen 7 (Right), depicting peak load (548,898 N) and modulus (38,390 MPa)

For Figures 4.11 and Figure 4.12, the capsular layers for SS and SC are presented. The overall shape of these graphs are much sharper at the centre than the bursal/tendinous and cadaveric layers, which gives an indication of the characteristics of the fibres found in the capsular layer. These layers present an even load/extension increase, with no exact yield strength point as it reaches peak load. There is also little to no "spikes" presented in the deformation of the layers and shows that these fibres are different than those in the bursal/tendinous layer as it would rather breakdown as one unit, instead of in "pieces" like the bursal/tendinous layer. These graphs then descend at a constant gradient as tissue degrades and weakens.

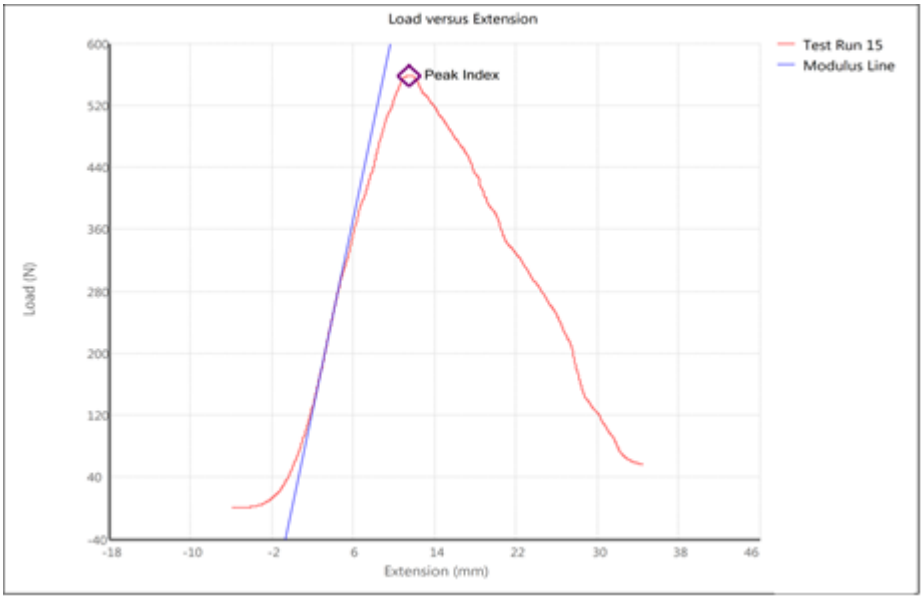

Figure 4.11 Load (N) versus extension (mm) graph for bursal specimen 10 (Right), depicting peak load (558,332 N) and modulus (47,112 MPa), Peak Load

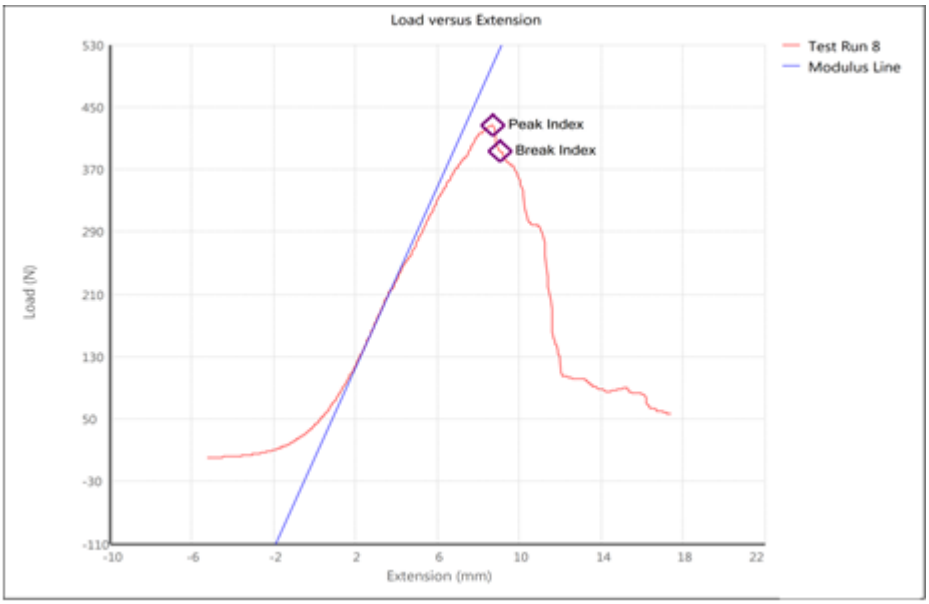

Figure 4.12 Load (N) versus extension (mm) graph for bursal specimen 9 (Left), depicting peak load (426,817 N) and modulus (44,384 MPa)

4.2 Testing for Normality

4.2.1 Tests for Normality for peak load (N) and modulus (MPa) for individual tendons

Peak load

Based on the normality tests which were done on the individual samples, the only sample that was not normally distributed for peak load (N) was the capsular SS layer (Table 4.7) and for the modulus, the bursal SC layer (Table 4.8). The rest of the data sets for all samples displayed normal distribution.

Table 4.7 Test for normality for the peak load (N) of supraspinatus (SS), infraspinatus (IS) and subscapularis (SC) in the cadaver, bursal and capsular samples *(* - indicating distribution that is not normal)*

Sample	N	Shapiro-Wilk	p-value
Cadaver SS	5	0,935	0,627
Bursal SS	12	0,927	0,349
Capsular SS*	*4*	*0,723*	*0,021**
Cadaver IS	5	0,970	0,872
Bursal IS	12	0,883	0,097
Capsular IS	4	0,879	0,333
Cadaver SC	4	0,984	0,927
Bursal SC	12	0,923	0,311
Capsular SC	5	0,928	0,583

Table 4.8 Test for normality for the modulus (MPa) of supraspinatus (SS), infraspinatus (IS) and subscapularis (SC) in the cadaver, bursal and capsular samples *(* - indicating distribution that is not normal)*

Sample	N	Shapiro-Wilk	p-value
Cadaver SS	5	0,944	0,695
Bursal SS	5	0,894	0,375
Capsular SS	4	0,868	0,288
Cadaver IS	3	0,867	0,287
Bursal IS	5	0,898	0,399
Capsular IS	4	0,802	0,107
Cadaver SC	4	0,773	0,062
Bursal SC*	*4*	*0,645*	*0,002**
Capsular SC	5	0,939	0,656

4.3 Comparative statistics

For the comparative statistics, a two sample t-test was used for all the normally distributed data in order to establish possible significant mean differences firstly, between the different tendons themselves in the same sample (i.e. cadaver SS vs cadaver IS; cadaver SS vs cadaver SC; cadaver IS vs cadaver SC; bursal SS vs bursal IS; bursal SS vs bursal SC; bursal IS vs bursal SC; capsular IS vs capsular SC) and secondly, between the different layers across samples (i.e. cadaver SS vs bursal SS; cadaver IS vs bursal IS; cadaver SC vs bursal SC; cadaver IS vs capsular IS; cadaver SC vs capsular SC; bursal IS vs capsular IS; bursal SC vs capsular SC) for peak load (N).

The same was conducted for the modulus (MPa) to determine differences firstly, between the different tendons themselves in the same sample (i.e. cadaver SS vs cadaver IS; cadaver SS vs cadaver SC; cadaver IS vs cadaver SC; bursal SS vs bursal IS; capsular SS vs capsular IS; capsular SS vs capsular SC; capsular IS vs capsular SC) and secondly, between the different layers across samples (i.e. cadaver SS vs bursal SS; cadaver IS vs bursal IS; cadaver SC vs bursal SC; cadaver IS vs capsular IS; cadaver SC vs capsular SC; bursal IS vs capsular IS; bursal SC vs capsular SC) for peak load (N). A p-value less than or equal to 0.05 is indicative that a significant difference exists between the sample means.

For the data that were not normally distributed, a Mann-Whitney U test was used to establish possible mean differences firstly, between the different tendons themselves in the same sample (i.e. bursal SS vs bursal SC; bursal IS vs bursal SC) and secondly, between the different layers across samples (i.e. cadaver SC vs bursal SC; capsular SC vs bursal SC) for both peak load (N) and modulus (MPa) as describe above. A p-value less than or equal to 0.05 is indicative that a significant difference exists between the sample means.

4.3.1 Two sample t-test for cadaver (SS, IS, SC), bursal (SS, IS, SC) and capsular (IS, SC) layers: peak load (N)

The only significant differences that were observed in this sample were between the cadaveric SS and bursal SS layers and between the cadaveric IS and bursal IS layers with regard to peak load (N). Table 4.16 highlights the significant difference (p=0.002) between the cadaveric SS and bursal SS layer. This is also shown by the big difference in the mean value of 548,21 N for the cadaveric SS and a lower 190.05 N value for the bursal SS layer. Table 4.17 highlights the significant differences (p=0.0003) between the cadaveric IS and bursal IS layers. The mean values for cadaveric IS layer amounts to 432.57 N, and a 171.13 N value for the bursal IS layer. Only the significant results are presented in this chapter while the rest of the results can be found in Appendix II

Table 4.9 Two sample t test for the cadaver SS vs bursal SS peak load (N)

Tests for equal means:

Cadaver SS		**Bursal SS**	
N:	5	**N:**	12
Mean:	548,21	**Mean:**	190,05
95% conf.:	(223,93 872,49)	**95% conf.:**	(104,19 275,91)
Variance:	68208	**Variance:**	18260

Difference between means:	358,16
95% conf. interval (parametric):	(156,54 559,78)
95% conf. interval (bootstrap):	(147,59 582,38)

t :	3,786	**p (same mean):**	0,002

Table 4.10 Two sample t test for the cadaver IS vs bursal IS peak load (N)

Tests for equal means:

Cadaver IS		**Bursal IS**	
N:	5	**N:**	12
Mean:	432,57	**Mean:**	171,13
95% conf.:	(137,95 727,18)	**95% conf.:**	(127,23 215,02)
Variance:	56300	**Variance:**	4772,9

Difference between means:	261,44
95% conf. interval (parametric):	(107,07 415,81)
95% conf. interval (bootstrap):	(85,424 458,94)

t :	3,610	**p (same mean):**	0,003

4.3.2 Two sample t-test for cadaver (SS, IS, SC), bursal (SS, IS, SC) and capsular (IS, SC) layers: modulus (MPa)

For the modulus of elasticity, there was only a significant difference shown between the cadaveric SS and bursal SS with a p-value of 0.033. The mean values for these two layer differ by 15.92, with the cadaveric SS layer being the highest at 31,45 MPa. Only the significant results are presented in this chapter, please see Appendix II for the rest of the results.

Table 4. 11 Two sample t test (test for equal means) – cadaver SS vs bursal SS modulus (MPa)

Tests for equal means

Cadaver SS		**Bursal SS**	
N:	5	**N:**	5
Mean:	31,45	**Mean:**	15,54
95% conf.:	(17,283 45,624)	**95% conf.:**	(5,903 25,167)
Variance:	130,24	**Variance:**	60,18

Difference between means:	15,92
95% conf. interval (parametric):	(1,6875 30,149)
95% conf. interval (bootstrap):	(5,217 26,864)

t :	2,579	**p (same mean):**	0,033
Uneq. var. t :	2,579	**p (same mean):**	0,036
Monte Carlo permutation:		**p (same mean):**	0,041
Exact permutation:		**p (same mean):**	0,044

4.3.3 Nonparametric data (not normally distributed): Modulus bursal SC

For the nonparametric data, the Mann-Whitney u test revealed a significant difference between the modulus property between the bursal SS and bursal SC layer, with a significant p-value of 0.020. The bursal SC had the highest mean rank value of 3.33, whereas the bursal SS layer equalled to 1.67.

Table 4.12 Mann-Whitney u test (test for equal medians) – bursal SS vs bursal SC modulus (MPa)

Tests for equal medians

Bursal SS		**Bursal SC**	
N:	5	**N:**	4
Mean rank:	1,67	**Mean rank:**	3,33

Mann-Whitn U :	0		
z :	-2,327	**p (same med.):**	0,020
Monte Carlo permutation:		**p (same med.):**	0,016
Exact permutation:		**p (same med.):**	0,016

A significant difference was also found between the modulus of bursal IS and bursal SC layer, with a significant p-value of 0.012. The Bursal SC had the highest Mean rank value of 3.33, whereas the bursal IS layer equalled to 1.67.

Table 4.13 Mann-Whitney u test (test for equal medians) – bursal IS vs bursal SC modulus (MPa)

Tests for equal medians

Bursal IS		**Bursal SC**	
N:	5	**N:**	4
Mean rank:	1,67	**Mean rank:**	3,33

Mann-Whitn U :	0		
z :	-2,327	**p (same med.):**	0,012
Monte Carlo permutation:		**p (same med.):**	0,0177
Exact permutation:		**p (same med.):**	0,016

Chapter 5: Discussion

Understanding the biomechanical properties of the RC have become a higher priority in current Orthopaedic research. Ultimately the main purpose of these surgeries is to successfully repair the RC tendons to restore as close to normal functionality back to RC. In essence, being able to restore functionality means understanding the intricate and complex nature of the biomechanical components and properties of the RC unit. Biomechanical studies investigating the pure tendon properties of the RC are therefore vital to contribute knowledge to the Orthopaedic community for the enhancement of surgical procedures.

5.1 Anisotropic nature of tendons

Anisotropic materials are said to have different physical and mechanical properties within the material itself and often differ with orientation, which can be seen in most biological materials like wood, tendons and bone (Miller, n.d.; Solid Mechanics Part I: An Introduction to Solid Mechanics, n.d.). These materials, like tendons have different mechanical properties within the same material, which includes having mechanically different directions, that is the reason why these materials don't have a clean break when tension is applied, but rather react independently within the material structure (Solid Mechanics Part I: An Introduction to Solid Mechanics). To fully appreciate the true reaction and display of material property of fresh and cadaveric tissue to load and extension is with a graph. Statistical methods comparing significance of the values do not always best represent the reaction of the tissue during the stresses placed upon it during testing, therefore graphs of force (N) over extension (mm) were also used during this study.

The graphs obtained in this study presented more valuable information than just the statistics and displayed the true nature of each layer and tendon; fresh or cadaveric. Looking only at the cadaveric graphs versus the bursal layer graphs, it is clear that these tendons reacted differently to load. This difference clearly highlights the influence the embalming chemicals have on the nature of the material of each individual tendon. The cadaveric graphs displayed a much higher peak load (N) than the fresh bursal/tendinous layer, but as shown in Figures 4.7 and 4.8, much less reaction from individual tissue fibres are found. In other words, the embalmed tendon tends to break up as a whole or more complete and with a longer extension before descending and breaking down completely. The fresh bursal/tendinous layer on the other hand breaks down in different sections even before reaching the peak load giving evidence to the fresh tissues anisotropic properties in that these fibres act independently depending on which direction the load is being applied. Therefore, before taking the significant statistical difference in account displayed by Table 4.16 and Table 4.17, it can be shown just by looking at the reaction of the tendons using the graphs that they react differently.

It is also important to look at the modulus of elasticity in these graphs and how the cadaver specimens react in comparison to the bursal/tendinous specimens. It is clear that the

bursal/tendinous layer displays a higher flexibility with evidence of the modulus being low. With regards to the cadaver specimens, the modulus is higher and therefore flexibility is lower. This makes sense due to the fixative nature of the embalming chemicals which will change the chemical make-up of the tendons making them more stiff and therefore reducing their flexibility.

5.2 Tensile properties of the RC tendons

In this study, strips of the bursal/tendinous and capsular layers were used. Studies using this method, cut the tendons in 25 mm strips in width (Nakajima *et al.,* 1994), and therefore the same method was used for best grip of the tendon (40 mm x 25mm). The results that were obtained included, the peak load in Newton force (N), which is the maximum tensile strength reached by the specimen. The tensile strength is defined as the resistance of the tendon to break under tension (pulling of the tendon). And another measurement that was also included was the elastic modulus or otherwise known as Young's Modulus, measured in MPa, which is the ratio of stress to correspond to strain in the tendon under tension (Kent, 2017). These two measurements were used to show the tensile biomechanical properties between the different sample sets and to compare the results with previous studies.

5.2.1. Peak load (N) to failure

Numerous experimental studies have been done to determine the biomechanical properties of the RC tendons (Clark *et al*., 1992; Itoi *et al*., 1995; Nimura *et al*., 2012; Nakajima *et al.,* 1994) and/or different surgical techniques (Klepps *et al*., 2004; Ghodadra *et al*., 2009; Behrens *et al*., 2011; Le *et al*., 2014), but the results of each study remain inconsistent. This is due to different methods used to test these tendons, like bone fixation of the tendons; using strips of tendons; using the complete RC unit etc. The results of tendon testing also varies due to the different experimental techniques used, such as static testing versus cyclic loading, using different time constraints (0.5mm/s versus 50mm/s) or have a preload of 10N versus a preload of 50N. Another component to consider is the availability of technology with regard to testing equipment and programming. In this study, the available technology allowed a simple load to failure technique to be used, gripping the two ends of the tendons or capsular layer to test the maximum tensile load it can withstand. This testing technique pulls the tendon in a single direction at a constant rate until failure, which reflects closer to a traumatic tear, than a degenerative tear.

Aside from the different experimental conditions, studies have shown vast differences in peak load to failure under specified conditions. Itoi et al. (1995) tested fresh cadaveric supraspinatus samples. The authors split the tendons into anterior and posterior strips and found that the anterior strips had an ultimate load of 411.1 N while the more posterior strips resulted in a much lower load of 88 N. Anatomically, the posterior strips would be those associated with the interdigitation with infraspinatus under and posterior to the spinoglenoid notch and therefore it makes sense that if the posterior strips were not tested while integrated

with infraspinatus, they would be compromised and therefore possibly produce a lower load to failure. The anterior strips may be stronger due to the gap between the interdigitating fibres of subscapularis via the bicipital groove. According to Nakajima et al. (1994), the ultimate load for their study using the SS layer (bursal/tendinous and capsular layer) was 9 N/mm^2 (+/- 91.8 N), almost an 8th compared to another known study done by Halder et al. (2000), which yielded 424.2 N from the IS superior strip and 406.9 N from the IS inferior strip. Other studies found the supraspinatus tendon to yield higher tensile loads of up to 784 N (Wilson and Duff, 1943) All the previous studies investigated the properties of fresh tissue and no study to the authors knowledge has investigated the biomechanical properties of embalmed human, rotator cuff tendons. In this study a sample of embalmed tissue was included to compare the effect that chemical intervention would have on the material property of the tendons. Looking at merely the mean value of the cadaveric versus the fresh specimens, it is evident that the cadaveric yielded a much higher peak load in all 3 layers, 548.2±261.2 N (SS), 432.6±237.3 N (IS) and 452.0±194.5 N (SC) (Tables 4.1,4.2 and 4.3), compared to the fresh specimens which showed the highest means in the bursal (SC) of 254.6±52.5 N (Table 4.3), the capsular IS of 203.9±39.4 N (Table 4.2) and in the SS capsular layer of 232.0±130.8 N (Table 4.1). What is interesting is that comparatively, the results of this study show much lower load to failure forces than the studies by Wilson and Duff (1943), Itoi et al (1995) and Halder et al. (2000), but higher values than those obtained in the study done by Nakajima et al. (1994). These inconsistencies may be due to the different experimental protocols employed by the various authors as well as the difference in sample demographics.

In general, these results firstly show that the embalming process definitely influences not only the appearance, but overall biomechanical properties of the RC tendons. The embalming process influences the fibre properties, which includes elasticity, flexibility, toughness, tensile strength and resistance to name a few (Wilke *et al*., 1996; Verstraete *et al*., 2014). These obvious changes influence the integrity of the cadaveric shoulders, specifically to be used for research in the biomechanical properties of the RC tendons. The results confirm that cadaveric specimens do not yield accurate representation results for RC tendons and should rather not be considered when studying the properties of true RC tendons as it can be misleading. Secondly, the results indicate the clear disparity between this studies outcomes and previous studies done in the past. Much can be attributed to this fact, as mentioned earlier, such as the varying and inconsistent experimental protocols used to test the tendons; whether the tendons were tested as a whole or separated into their bursal/tendinous and capsular layers; whether the tendons were attached to the bone during testing or as separate structures and then lastly the demographics may have an influence on the material properties and therefore these elements are aspects that require further investigation.

5.2.2 Modulus of elasticity of tendons

Although the Modulus (MPa) results were not initially part of the study outcomes, it was included for future research purposes. During the development of research in biomechanical properties of the RC, it is important to consider every composition and characteristic that makes up the function of these layers of the RC complex. One of them

being the Modulus of elasticity (MPa), which is defined as the ratio of stress corresponding to strain in the tendon under tension (Kent, 2017). The modulus of elasticity basically gives an indication as to the stiffness of the material, which is also explained by using the term flexibility. Unfortunately, only limited data could be used for the modulus results due to technical problems arising during the project (addressed in limitations), but it still gives an indication that is worth researching further. The modulus is definitely an interesting component that can be looked at in future studies.

The results obtained for the highest average modulus was as follow: capsular SS layer with averages of 27.4±5.9 MPa (Table 4.4), in the cadaver specimens IS with an average of 47.2±26.3 MPa (Table 4.5) and for the bursal layer SC with average of 79.3±41.0 MPa (Table 4.6). The lowest average modulus values were as follow: cadaver SS layer with an average of 1.45±5.1 MPa (Table 4.4), the bursal IS layer with an average of 11.53±3.7 MPa (Table 4.5) and the capsular SC layer with an average of 0.92±7.5 MPa (Table 4.6). Therefore, the layers representing the most flexibility during this study were the layers with the lowest MPa value. Looking at the results, the most elastic layers would have been the capsular SC layer. For the tendons which had a modulus value, there was a difference observed between the bursal SS vs bursal SC modulus (MPa), indicating a p-value of 0.020 MPa (Table 4.42) and for bursal IS vs bursal SC modulus (MPa) a p-value of 0.012 MPa (Table 4.43). This indicates a difference of Modulus of elasticity between the sections within the bursal layer and should be considered during future studies. The results obtained for this section of the work are quite contradicting to what is expected, which is that the most elastic layer should be the bursal/tendinous layer in general. Unfortunately, due to the sparse amount of specimen data, these results cannot be confirmed and do need to be further investigated.

5.3 Biomechanical comparisons between the bursal/tendinous and capsular layers

During the dissection of the fresh specimens the different layers were clearly observed, namely the bursal/tendinous (outer) later and the capsular (inner) layer. These two layers as shown in previous studies are separate, but interdigitate with one another at the point of insertion into the tubercles and was once again confirmed during this study (Clark *et al.*, 1992; Nakajima *et al.*, 1994). It was also noted the difference in fibre direction and composition, specifically looking at the difference in the graphs.

The descriptive statistics showed that the mean peak load to failure for SS and IS in the capsular layer was higher (232.0±65.4 N and 203.9±39.6 N, respectively) than the SS and IS in the bursal layer (190.1±39.0 N and 171.1±19.9 N, respectively). Interestingly for SC, the bursal layer displayed a slightly higher peak load (254.6±52.5 N) than the capsular layer (244.9±95.7 N). Although the differences did not come up as significant, the mean values did show variances which could be due to several reasons. The first could be due to the number of samples tested, as more specimens were available for the bursal/tendinous layer than the capsular layer. It can also be due to the age of the individuals, from natural deterioration and

overuse. Even though the bursal/tendinous and capsular layer did not show a significant peak load (N) difference, the physical reaction due to force did show a difference and this was illustrated by the load versus extension graphs discussed in Section 5.1.

The SS and IS bursal layer showed a lower modulus (higher flexibility) overall (15.5±3.5 MPa and 11.5±3.7 MPa, respectively) compared to the capsular SS (27.4±5.9 MPa) and IS (23.5±8.5 MPa). Once again, the vice versa was noted for the bursal versus capsular layer for the SC tendon, where the capsular showed a lower modulus (0.9±7.5 MPa) than the bursal layer (79.3±41.0 MPa), indicating that the capsular layer for SC has more flexibility than the bursal layer. This could be due to the fact that the SC has a more tendinous area superiorly, which forms part of the bicep tendon, and also due to fibres running horizontally, instead of more longitudinally (Kircher *et al,*. 2015). It is also known that an interdigitation exist between the fibers of the coracohumeral ligament and the superior SC tendon, which could be the reason for reduced flexibility and increase in the peak load value for the bursal layer of the SC (Petchprapa *et al.,* 2010).

Referring back to the bursal graphs, the bursal/tendinous layer presented "spikes" as force was applied, showing the individual properties of the fibres presented in this layer and how they break down in sections, instead of a complete rupture of the sample. In the study done by Nakajima et al. (1994), the bursal/tendinous layer could disperse the force applied and create more resistance, which then causes a greater elongation (flexibility) of the layer. The bursal/tendinous layer is also thicker than the capsular layer and contains some muscular fibres, which were more in some individuals and less in others and could also be a factor to consider when comparing the peak loads. Whereas the capsular layer graphs display little to no "spikes", which confirms the possibility of the fibres reacting in a unified way, instead of individually and breaks down faster as a whole. This layer also had no muscular fibres and are presented as part of the joint capsule, which comprises of a more cartilaginous tissue.

The physical composition of the capsular layer can be described as a mesh-like, fibrous tissue, which makes it much more ridged, which has a greater possibility of rupturing. Looking at the physical reaction and not just the peak load, gives a clearer understanding of the function and characteristics of these two layers and should still be regarded as biomechanically different layers.

Further studies should be considered to study every aspect of the biomechanical properties, to give a clearer understanding to why these two layers' function and react so different in the event of an injury or deterioration.

5.4 General

The results obtained in this study not only gives insight into the overall biomechanical properties of the RC tendons capsular and bursal/tendinous layers, but more importantly the results have the potential to influence the surgical procedures for RC surgery and ultimately, the outcomes of RC repairs (De Beer, *per comm;* Nakajima *et al.,* 1994). Looking at the peak loads, surgeons are able to understand the strength of the tendons, but more importantly, the

difference in layers of the RC complex. These results show and provide evidence that a difference between the bursal/tendinous layer and the capsular layer exist and should be a noteworthy consideration during surgical repair in the fact that these two layers should be treated as separately functioning layers. Not only do these two layers have different fibre properties, which includes elasticity, collagen fibres and connective tissue arrangement, but these two layers' function together, as well as independently. This is what makes it one of the most unique, yet complex tissues in the body, but also gives it its strength and function.

Too many RC surgeries fail due to a misunderstanding of the properties of the RC complex, which is mostly a result of surgeons not taking in consideration the bursal/tendinous and capsular layers. In many cases patient's symptoms present a tear, but no evidence is shown during the routine scans or consultations, which in many cases are related to an "underlying" capsular tear and are usually misdiagnosed by physicians. These tears then usually result in massive/full thickness tears which includes the bursal/tendinous layer. These massive tears are mostly a result of misinterpretation, which is evidently a result of not knowing the correct properties and anatomy of the RC complex.

5.5 Limitations

As this is an experimental study with many uncontrollable aspects, several limitations were found for this study.

- Great quality specimen availability was limited and therefore in some instances, equal numbers of sample testing could not be achieved. The capsular layer was a difficult region to dissect out and therefore only 5could be tested, compared to the bursal/tendinous layer where 12specimens could be harvested. This unequal sample size is a limitation especially for comparative purposes.
- For the study purpose, the tendons were cut into separate pieces and removed from their insertions on the humeral tubercles. This complete removal could possibly lead to additional weakening of the tendons themselves as they do not present in their anatomic position and condition.
- The individual testing of the strips of tendons only gives an estimate and may influence the total sum of the tensile strength.
- At first the ridged/tooth-like clamps were tested during the initial experimental trial, but failed to hold the strips. The second approach was more successful, using the normal rubber clamps and reinforcing the grips with sand paper. This allowed a better grip on the tendons and better results were obtained, although there was still a number of tendons that slipped.
- Another limitation that involved the grips was the point of strain on the tendon. Some of the tendons tore at/near the grip site of the tendon as this posed a spot of weakness created artificially by the position of the hard metal clamp. Methods to overcome this

problem include using cryoclamps, but unfortunately this is a very expensive option and is not available in SA at the moment.

Chapter 6: Conclusion

Throughout the study it has been evident that all structures forming part of the RC are important in the functioning of the RC complex. Previous studies have shown the RC tendons to function together, but still have individual functions within the separate tendons and their layers (Clark *et al.*, 1992; Itoi *et al*., 1995). The RC bursal/tendinous layer and capsular layer cannot be treated as the same layer or structure, instead through the results obtained it is clear that these layers do in fact show different functional properties More importantly, the physical reaction when force is applied has shown to be more reliable than simply looking at the statistical values. It was evident that during these tests, the capsular layer overall was less elastic than the bursal/tendinous layer, due to the difference in the molecular make up of these individual layers. It also showed clearly that using cadaveric specimens for accurate realistic results is not reliable, due to the molecular change that takes place because of the embalming process.

It is important to study the histological properties of these layers separately as well as combined (where these layers interdigitate) to understand the underlying function of the fibres within these layers. This includes defining the molecular make up for each structure as well as the direction of these fibres within the layer. It is evident that other structures, including the coracohumeral ligament, the coracoacromial ligament, the long head of bicep tendons and all other layers of tendon, ligament and muscles around and part of the RC complex, play a vital part in this mechanism and its function. More emphasis should also be placed on the different biomechanical properties, like stress, strain, elasticity and displacement. These properties greatly define the layers of the RC in more depth, to better understand how this mechanism function and more importantly how it can be repaired to restore its original function.

As seen in the literature for this study, there is very little evidence supporting the fact that the RC complex has different layers and different functions in these layers. This is the reason for many undiagnosed or misdiagnosed RC tears. Most of the tears that occur in the capsular layer are missed during consultations, tests and even during surgeries. Therefore, more tests and observation should be made to correctly diagnose these tears to prevent a full thickness tear or other RC complications.

Future recommendations

Taking all the different studies and methods used to test the RC complex, it is clear that there is still a lot of opportunity to do more research and discover more about the function and anatomy of this mechanism. Referring back to this study alone opened up more doors for future research, specifically to the methods of testing the different layers of the RC, which will assist in eliminating or decreasing the limitations. There are very few studies that discuss these two layers in detail and much more is needed to fully comprehend the biomechanical properties, as well as function of them separate and functioning together. This is also shown to be vitally important during surgery and how surgeons can be made more

aware of these differences and incorporate that in their surgeries to give the best possible outcome for the patient.

Not much emphasis was put on the modulus of elasticity at the beginning of this study, but as the study developed, it was discovered that this could be an important part to consider for future studies and for the function of the RC complex. Future studies can focus on the modulus as well as the stress strain and displacement of the tendon. This will bring the focus more towards the physical reaction of the tendons which would be beneficial during surgeries and for the rehabilitation of the RC complex.

Chapter 7: References

Adams, C., DeMartino, A., Rego, G., Denard, P. and Burkhart, S. (2016). The Rotator Cuff and the Superior Capsule: Why We Need Both. *Arthroscopy: The Journal of Arthroscopic & Related Surgery*, 32(12), pp.2628-2637.

Ahmad, S., Haber, M. and Bokor, D. (2015). The influence of intraoperative factors and postoperative rehabilitation compliance on the integrity of the rotator cuff after arthroscopic repair. *Journal of Shoulder and Elbow Surgery*, 24(2), pp.229-235.

Aleem, A. and Brophy, R. (2012). Outcomes of Rotator Cuff Surgery. *Clinics in Sports Medicine*, 31(4), pp.665-674.

Aramberri-Gutiérrez, M., Martínez-Menduiña, A., Valencia-Mora, M. and Boyle, S. (2015). All-Suture Transosseous Repair for Rotator Cuff Tear Fixation Using Medial Calcar Fixation. *Arthroscopy Techniques*, 4(2), pp.e169-e173.

Bailie, D. and Ellenbecker, T. (2009). Severe chondrolysis after shoulder arthroscopy: A case series. *Journal of Shoulder and Elbow Surgery*, 18(5), pp.742-747.

Belangero, P., Ejnisman, B. and Arce, G. (2013). *Shoulder Concepts 2013: Consensus and Concerns*. 1st ed. Berlin, Heidelberg: Springer Berlin Heidelberg, pp.5-13.

Behrens, S., Bruce, B., Zonno, A., Paller, D. and Green, A. (2011). Initial Fixation Strength of Transosseous-Equivalent Suture Bridge Rotator Cuff Repair Is Comparable With Transosseous Repair. *The American Journal of Sports Medicine*, 40(1), pp.133-140.

Bishop, J., Klepps, S., Lo, I., Bird, J., Gladstone, J. and Flatow, E. (2006). Cuff integrity after arthroscopic versus open rotator cuff repair: A prospective study. *Journal of Shoulder and Elbow Surgery*, 15(3), pp.290-299.

Bitar, A., Santos, L., Croci, A., Pereira, J., França Bisneto, E., Giovani, A. and Oliveira, C. (2010). Histological study of fresh versus frozen semitendinous muscle tendon allografts. *Clinics*, 65(3).

Black, E., Lin, A., Srikumaran, U., Jain, N. and Freehill, M. (2015). Arthroscopic Transosseous Rotator Cuff Repair: Technical Note, Outcomes, and Complications. *Orthopedics*, 38(5), pp.e352-e358.

Blevins, F. (1997). Rotator Cuff Pathology in Athletes. *Sports Medicine*, 24(3), pp.205-220.

Burkhead, W., Skedros, J., ORourke, P., Pierce, W. and Pitts, T. (2007). A Novel Double-row Rotator Cuff Repair Exceeds Strengths of Conventional Repairs. *Clinical Orthopaedics and Related Research*, PAP.

Chaudhury, S., Holland, C., Thompson, M., Vollrath, F. and Carr, A. (2012). Tensile and shear mechanical properties of rotator cuff repair patches. *Journal of Shoulder and Elbow Surgery*, 21(9), pp.1168-1176.

Clark JM, Harryman DT. (1992). Tendons, ligaments, and capsule of the rotator cuff. *The Journal of Bone and Joint surgery*, incorporated, 74-A, pp.713-725

Chansky, H. and Iannotti, J. (1991). The vascularity of the rotator cuff. *Journal of Clinical Sports Medicine*, 10(4), pp.807-822.

Chow, M. and Zhang, Y. (2011). Changes in the Mechanical and Biochemical Properties of Aortic Tissue due to Cold Storage. *Journal of Surgical Research*, 171(2), pp.434-442.

Cummins, C. and Murrell, G. (2003). Mode of failure for rotator cuff repair with suture anchors identified at revision surgery. *Journal of Shoulder and Elbow Surgery*, 12(2), pp.128-133.

Curtis, A., Burbank, K., Tierney, J., Scheller, A. and Curran, A. (2006). The Insertional Footprint of the Rotator Cuff: An Anatomic Study. *Arthroscopy: The Journal of Arthroscopic & Related Surgery*, 22(6), pp.603-609.e1.

Datavizcatalogue.com. (2018). *Box and Whisker Plots - Learn about this chart and its tools*. [online] Available at: https://datavizcatalogue.com/methods/box_plot.html

Davidson, J. and Burkhart, S. (2010). The Geometric Classification of Rotator Cuff Tears: A System Linking Tear Pattern to Treatment and Prognosis. *Arthroscopy: The Journal of Arthroscopic & Related Surgery*, 26(3), pp.417-424.

Dilisio, M., Noble, J., Bell, R. and Noel, C. (2013). Postarthroscopic Humeral Head Osteonecrosis Treated With Reverse Total Shoulder Arthroplasty. *Orthopedics*, 36(3), pp.e377-e380.

Fealy, Stephen, Ronald S. Adler, Marc C. Drakos, Anne M. Kelly, Answorth A. Allen, Frank A. Cordasco, and Stephen J. O'brien. (2006). "Patterns of Vascular and Anatomic Response Following Rotator Cuff Repair (SS-34)." Arthroscopy: *The Journal of Arthroscopic & Related Surgery*: 27-28.

Fenwick, S., Hazleman, B. and Riley, G. (2002). The vasculature and its role in the damaged and healing tendon. *Arthritis Research*, 4(4), pp.252-260.

Franceschi, F., Ruzzini, L., Longo, U., Martina, F., Zobel, B., Maffulli, N. and Denaro, V. (2007). Equivalent Clinical Results of Arthroscopic Single-Row and Double-Row Suture Anchor Repair for Rotator Cuff Tears: A Randomized Controlled Trial. *The American Journal of Sports Medicine*, 35(8), pp.1254-1260.

Gamradt, S., Gallo, R., Adler, R., Maderazo, A., Altchek, D., Warren, R. and Fealy, S. (2010). Vascularity of the supraspinatus tendon three months after repair: Characterization using contrast-enhanced ultrasound. *Journal of Shoulder and Elbow Surgery*, 19(1), pp.73-80.

Gerber, C., Schneeberger, A., Beck, M. and Schlegel, U. (1994). Mechanical strength of repairs of the rotator cuff. *The Journal of Bone and Joint Surgery. British volume*, 76-B(3), pp.371-380.

Ghasemi, A. and Zahediasl, S. (2012). Normality Tests for Statistical Analysis: A Guide for Non-Statisticians. *International Journal of Endocrinology and Metabolism*, 10(2), pp.486-489.

Ghodadra, N., Provencher, M., Verma, N., Wilk, K. and Romeo, A. (2009). Open, Mini-open, and All-Arthroscopic Rotator Cuff Repair Surgery: Indications and Implications for Rehabilitation. *Journal of orthopaedic & sports physical therapy*, 39(2), pp.81-A6.

Goodmurphy, C., Osborn, J., Akesson, E., Johnson, S., Stanescu, V. and Regan, W. (2003). An immunocytochemical analysis of torn rotator cuff tendon taken at the time of repair. *Journal of Shoulder and Elbow Surgery*, 12(4), pp.368-374.

Goto, M., Gotoh, M., Mitsui, Y., Okawa, T., Higuchi, F. and Nagata, K. (2013). Rapid collapse of the humeral head after arthroscopic rotator cuff repair. *Knee Surgery, Sports Traumatology, Arthroscopy*, 23(2), pp.514-516.

Greenspoon, J., Petri, M. and Millett, P. (2016). Arthroscopic Knotless, Double-Row, Extended Linked Repair for Massive Rotator Cuff Tears. *Arthroscopy Techniques*, 5(1), pp.e127-e132.

Halder, A., Zobitz, M., Schultz, F. and An, K. (2000). Mechanical properties of the posterior rotator cuff. Clinical Biomechanics, 15(6), pp.456-462.

Habermeyer, P., Magosch, P. and Lichtenberg, S. (2006). *Classifications and scores of the shoulder*. Berlin: Springer, pp.165-169.

Hegedus, E., Cook, C., Brennan, M., Wyland, D., Garrison, J. and Driesner, D. (2009). Vascularity and tendon pathology in the rotator cuff: a review of literature and implications for rehabilitation and surgery. *British Journal of Sports Medicine*, 44(12), pp.838-847.

Huang, C., Wang, V., Pawluk, R., Bucchieri, J., Levine, W., Bigliani, L., Mow, V. and Flatow, E. (2005). Inhomogeneous mechanical behavior of the human supraspinatus tendon under uniaxial loading. *Journal of Orthopaedic Research*, 23(4), pp.924-930.

Hussey, M., Steen, B. and Frankle, M. (2016). *Reverse Shoulder Arthroplasty for Proximal Humerus Fractures*. [online] Musculoskeletal Key. Available at: https://musculoskeletalkey.com/reverse-shoulder-arthroplasty-for-proximal-humerus-fractures/ [Accessed 2018].

Itoi, E., Berglund, L., Grabowski, J., Schultz, F., Growney, E., Morrey, B. and An, K. (1995). Tensile properties of the supraspinatus tendon. *Journal of Orthopaedic Research*, 13(4), pp.578-584.

Kang, L., Henn, R., Tashjian, R. and Green, A. (2007). Early Outcome of Arthroscopic Rotator Cuff Repair: A Matched Comparison With Mini-Open Rotator Cuff Repair. *Arthroscopy: The Journal of Arthroscopic & Related Surgery*, 23(6), pp.573-582.e2.

Kent, M., 2017. Oxford University Press. *The Oxford Dictionary of Sports Science & Medicine*.

Khan Academy. (2018). *Khan Academy*. [online] Available at: https://www.khanacademy.org

Kim, D., ElAttrache, N., Tibone, J., Jun, B., DeLaMora, S., Kvitne, R. and Lee, T. (2006). Biomechanical Comparison of a Single-Row Versus Double-Row Suture Anchor Technique for Rotator Cuff Repair. *American Journal of Sports Medicine*, 34(3), pp.407-414.

Kim, K., Rhee, K., Shin, H. and Kim, Y. (2008). Arthroscopic Transosseous Rotator Cuff Repair. *Orthopaedics*, 31(4), pp.327-330.

Kircher, J., Schwalba, K. and Hedtmann, A. (2015). The Subscapularis Interlocking Stitch for the Arthroscopic Treatment of Subscapularis Tendon Tears at the Shoulder. *Arthroscopy Techniques*, 4(5), pp.e531-e535.

Klepps, S., Bishop, J., Lin, J., Cahlon, O., Strauss, A., Hayes, P. and Flatow, E. (2004). Prospective Evaluation of the Effect of Rotator Cuff Integrity on the Outcome of Open Rotator Cuff Repairs. *American Journal of Sports Medicine*, 32(7), pp.1716-1722.

Kokmeyer, D., Dube, E. and Millett,, P. (2016). Prognosis Driven Rehabilitation After Rotator Cuff Repair Surgery. *The Open Orthopaedics Journal*, 10(Suppl 1: M10), pp.339-348.

Kuroda, S., Ishige, N. and Mikasa, M. (2013). Advantages of Arthroscopic Transosseous Suture Repair of the Rotator Cuff without the Use of Anchors. *Clinical Orthopaedics and Related Research®*, 471(11), pp.3514-3522.

Lake, S., Miller, K., Elliott, D. and Soslowsky, L. (2009). Effect of fiber distribution and realignment on the nonlinear and inhomogeneous mechanical properties of human supraspinatus tendon under longitudinal tensile loading. *Journal of Orthopaedic Research*, 27(12), pp.1596-1602.

Le, B., Wu, X., Lam, P. and Murrell, G. (2014). Factors Predicting Rotator Cuff Retears: An Analysis of 1000 Consecutive Rotator Cuff Repairs. *The American Journal of Sports Medicine*, 42(5), pp.1134-1142

Lewis, J. (2009). Rotator cuff tendinopathy. *British Journal of Sports Medicine*, 43(4), pp.236-241.

Liu, S. and Baker, C. (1994). Arthroscopically assisted rotator cuff repair: Correlation of functional results with integrity of the cuff. *Arthroscopy: The Journal of Arthroscopic & Related Surgery*, 10(1), pp.54-60.

Ling, S., Chen, C. and Wan, R. (1990). A study on the vascular supply of the supraspinatus tendon. *Surgical and Radiologic Anatomy*, 12(3), pp.161-165.

Mall, N., Tanaka, M., Choi, L. and Paletta, G. (2014). Factors Affecting Rotator Cuff Healing. *The Journal of Bone & Joint Surgery*, 96(9), pp.778-788.

Mayoclinic.org. (2016). *Avascular necrosis - Mayo Clinic*. [online] Available at: http://www.mayoclinic.org/diseases-conditions/avascular-necrosis/basics/definition/CON-20025517 [Accessed 26 Oct. 2016].

Miller, N. (n.d.). *Isotropy: Definition & Materials | Study.com*. [online] Study.com. Available at: https://study.com/academy/lesson/isotropy-definition-materials.html.

Millstein, E. and Snyder, S. (2003). Arthroscopic management of partial, full-thickness, and complex rotator cuff tears: indications, techniques, and complications. *Arthroscopy: The Journal of Arthroscopic & Related Surgery*, 19(10), pp.189-199.

Mochizuki, T., Sugaya, H., Uomizu, M., Maeda, K., Matsuki, K., Sekiya, I., Muneta, T. and Akita, K. (2008). Humeral Insertion of the Supraspinatus and Infraspinatus. New Anatomical Findings Regarding the Footprint of the Rotator Cuff: Surgical Technique. *Journal of Bone and Joint Surgery. Essential Surgical Techniques*, os- 91(Supplement_2_Part_1), pp.1-7.

Naidoo, N., Lazarus, L., De Gama, B., Ajayi, N. and Satyapal, K. (2014). Arterial Supply to the Rotator Cuff Muscles. *Int. Journal Morphology.*, 32(1), pp.136-140.

Nakajima, T., Rokuuma, N., Hamada, K., Tomatsu, T. and Fukuda, H. (1994). Histologic and biomechanical characteristics of the supraspinatus tendon: Reference to rotator cuff tearing. *Journal of Shoulder and Elbow Surgery*, 3(2), pp.79-87.

Nimura, A., Kato, A., Yamaguchi, K., Mochizuki, T., Okawa, A., Sugaya, H. and Akita, K. (2012). The superior capsule of the shoulder joint complements the insertion of the rotator cuff. *Journal of Shoulder and Elbow Surgery*, 21(7), pp.867- 872. 16

Nho, S., Yadav, H., Shindle, M. and MacGillivray, J. (2008). Basic Science Update: Rotator Cuff Degeneration. *The American Journal of Sports Medicine*, 36(5), pp.987-993.

Panjabi, M., Krag, M., Summers, D. and Videman, T. (1985). Biomechanical time-tolerance of fresh cadaveric human spine specimens. *Journal of Orthopaedic Research*, 3(3), pp.292-300.

Papakonstantinou, M., Pan, W., le Roux, C. and Richardson, M. (2012). Arterial supply of the tendinous rotator cuff insertions: an anatomical study. *ANZ Journal of Surgery*, 82(12), pp.928-934.

Pandey, V. and Jaap Willems, W. (2015). Rotator cuff tear: A detailed update. *Asia Pacific Journal of Sports Medicine, Arthroscopy, Rehabilitation and Technology*, 2(1), pp.1-14.

Parada, S., Dilisio, M. and Kennedy, C. (2014). Management of complications after rotator cuff surgery. *Current Reviews in Musculoskeletal Medicine*, 8(1), pp.40-52.

Park, M., Tibone, J., ElAttrache, N., Ahmad, C., Jun, B. and Lee, T. (2007). Part II: Biomechanical assessment for a footprint-restoring transosseous-equivalent rotator cuff repair technique compared with a double-row repair technique. *Journal of Shoulder and Elbow Surgery*, 16(4), pp.469-476.

Petchprapa, C., Beltran, L., Jazrawi, L., Kwon, Y., Babb, J. and Recht, M. (2010). The Rotator Interval: A Review of Anatomy, Function, and Normal and Abnormal MRI Appearance. *American Journal of Roentgenology*, 195(3), pp.567-576.

Pouliart, N. and Gagey, O. (2006). Simulated humeral avulsion of the glenohumeral ligaments: A new instability model. *Journal of Shoulder and Elbow Surgery*, 15(6), pp.728-735.

Randelli, P., Spennacchio, P., Ragone, V., Arrigoni, P., Casella, A. and Cabitza, P. (2011). Complications associated with arthroscopic rotator cuff repair: a literature review. *Musculoskelet Surg*, 96(1), pp.9-16.

Rathbun, J. and Macnab, I. (1970). The microvascular of pattern of the rotator cuff. *The Bone and Joint Journal*, 52(3), pp.540-53.

Seida, J., Schouten, J., Mousavi, S., Tjosvold, L., Vandermeer, B., Milne, A., Bond, K., Hartling, L., LeBlanc, C. and Sheps, D. (2010). *Comparative effectiveness of nonoperative and operative treatments for rotator cuff tears*. 1st ed. Rockville, MD: Agency for Healthcare Research and Quality.

Seitz, A., McClure, P., Finucane, S., Boardman, N. and Michener, L. (2011). Mechanisms of rotator cuff tendinopathy: Intrinsic, extrinsic, or both. *Clinical Biomechanics*, 26(1), pp.1-12.

Solid Mechanics Part I: An Introduction to Solid Mechanics. (n.d.). [ebook] pp.126-131. Available at: http://homepages.engineering.auckland.ac.nz/~pkel015/SolidMechanicsBooks/index.html

Sugaya, H., Maeda, K., Matsuki, K., & Moriishi, J. (2007). Repair Integrity and Functional Outcome after Arthroscopic Double-Row Rotator Cuff Repair. A Prospective Outcome Study. *The Journal of Bone and Joint Surgery (American)*, 89(5), pp.953–960.

Thakkar, R., Thakkar, S., Srikumaran, U., McFarland, E. and Fayad, L. (2014). Complications of rotator cuff surgery—the role of post-operative imaging in patient care. *The British Journal of Radiology*, 87(1039), p.20130630.

Tham, E., Briggs, L. and Murrell, G. (2013). Ultrasound changes after rotator cuff repair: is supraspinatus tendon thickness related to pain?. *Journal of Shoulder and Elbow Surgery*, 22(8), pp.e8-e15.

www.dictionary.com. (2018). *the definition of biomechanical*. [online] Available at: https://www.dictionary.com/browse/biomechanical [Accessed 15 Aug. 2018].

Venkatasubramanian, R., Grassl, E., Barocas, V., Lafontaine, D. and Bischof, J. (2006). Effects of Freezing and Cryopreservation on the Mechanical Properties of Arteries. *Annals of Biomedical Engineering*, 34(5), pp.823-832.

Verstraete, M., Van Der Straeten, C., De Lepeleere, B., Opsomer, G., Van Hoof, T. and Victor, J. (2014). The effect of thiel embalming or dehydration on biomechanical properties of tendon, compared to fresh frozen tendons. Unpublished MMed dissertation. Faculty of Medicine of Ghent University, Ledeganck.

Vosloo, M., Keough, N. and De Beer, M. (2017). The clinical anatomy of the insertion of the rotator cuff tendons. *European Journal of Orthopaedic Surgery & Traumatology*, [online] 27(3), pp.359-366.

Waltrip, R., Zheng, N., Dugas, J. and \Andrews, J. (2003). Rotator cuff repair - A Biomechanical Comparison of Three Techniques. *American Journal of Sports Medicine*, 31(4), pp. 493-497

Weber, J., Agur, A., Fattah, A., Gordon, K. and Oliver, M. (2015). Tensile mechanical properties of human forearm tendons. *The Journal of Hand Surgery*, 40E(7), pp.711– 719.

Wildemann, B. and Klatte, F. (2012). Biological aspects of rotator cuff healing. *Journal of Muscles Ligaments Tendons*, 1(4), pp.161-168.

Wilke, H., Krischak, S. and Claes, L. (1996). Formalin fixation strongly influences biomechanical properties of the spine. Journal of Biomechanics, 29(12), pp.1629- 1631.

Wilson, C. and Duff, G. (1943). Pathologic study of degeneration and rupture of the supraspinatus tendon. Archives of Surgery, 47(2), p.121.

Yeh, P. and Kharrazi, F. (2012). Postarthroscopic Glenohumeral Chondrolysis. *Journal of the American Academy of Orthopaedic Surgeons*, 20(2), pp.102-112.

Appendix I: Raw data

Total Cadaveric Specimen data

Cadaveric SS						
Sample number	**Shoulder side**	**Force (N)**	**Modulus (Mpa)**	**Ethnicity**	**Age**	**Sex**
7288	Right	811,508	31,209	White	78	Male
7288	Left	778,03	41,083	White	78	Male
7263	Right	415,372	26,454	White	34	Female
7263	Left	552,656	15,232	White	34	Female
7198	Right	183,489	43,288	White	82	Female
Cadaveric IS						
Sample number	**Shoulder side**	**Force (N)**	**Modulus (Mpa)**	**Ethnicity**	**Age**	**Sex**
7288	Right	693,97		White	78	Male
7288	Left	591,087	99,165	White	78	Male
7263	Right	468,903		White	34	Female
7263	Left	319,173	14,450	White	34	Female
7198	Right	89,696	28,087	White	82	Female
Cadaveric SC						
Sample number	**Shoulder side**	**Force (N)**	**Modulus (Mpa)**	**Ethnicity**	**Age**	**Sex**
7288	Right	475,766	10,971	White	78	Male
7288	Left	691,865	48,586	White	78	Male
7263	Left	421,829	14,520	White	34	Female
7198	Right	218,715	17,663	White	82	Female

Total Bursal Fresh Specimen data

Fresh SS Bursal						
Sample number	**Shoulder side**	**Force (N)**	**Modulus (Mpa)**	**Ethnicity**	**Age**	**Sex**
1	Right	352,554	10,027	White	64	Male
1	Left			White	64	Male
2	Right	31,65		White	76	Female
2	Left	11,62		White	76	Female
3	Right	268,94		White	54	Male
3	Left	216,897	20,921	White	54	Male
4	Left	242,12		White	67	Male
5	Right	190,09		White	77	Male
6	Left	46,09		White	83	Male
7	left	223,405		White	59	Male
7	Right	446,8	18,98	White	59	Male
8	Left	48,718	4,819	White	58	Female
Fresh IS Bursal						
Sample number	**Shoulder side**	**Force (N)**	**Modulus (Mpa)**	**Ethnicity**	**Age**	**Sex**
1	Right	231,371	6,457	White	64	Male
1	Left	114,27		White	64	Male
2	Right	74,26		White	76	Female
2	Left			White	76	Female
3	Right	254,32		White	54	Male
3	Left	152,452	3,421	White	54	Male
4	Left	242,121		White	67	Male
5	Right	74,23		White	77	Male
6	Left	86,04		White	83	Male
7	left	219		White	59	Male
7	Right	183,758	11,83	White	59	Male
8	Left	240,086	11,152	White	58	Female
8	Right	181,645	24,78	White	58	Female
Fresh SC Bursal						
Sample number	**Shoulder side**	**Force (N)**	**Modulus (Mpa)**	**Ethnicity**	**Age**	**Sex**
1	Right	130,823	202,415	White	64	Male
1	Left			White	64	Male
2	Right	276,01		White	76	Female
2	Left	45,71		White	76	Female
3	Right	498,4		White	54	Male
3	Left	98,439	39,766	White	54	Male
4	Left	229,61		White	67	Male
5	Right	140,79		White	77	Male

6	Left	83		White	83	Male
7	left	397,392		White	59	Male
7	Right	548,898	38,390	White	59	Male
8	Right	351,647	36,685	White	58	Female

Total Capsular specimen data

Fresh SS Capsular						
Sample number	**Shoulder side**	**Force (N)**	**Modulus (Mpa)**	**Ethnicity**	**Age**	**Sex**
9	Left	426,817	44,384	White	64	Male
9	Right	188,244	16,894	White	64	Male
10	Right	159,348	24,786	White	54	Male
11	Right	153,643	23,564	White	55	Male
Fresh IS Capsular						
Sample number	**Shoulder side**	**Force (N)**	**Modulus (Mpa)**	**Ethnicity**	**Age**	**Sex**
9	left	108,146	16,649	White	64	Male
9	Right	271,872	18,24	White	64	Male
10	Right	265,919	48,491	White	54	Male
11	Right	169,837	10,436	White	55	Male
Fresh SC Capsular						
Sample number	**Shoulder side**	**Force (N)**	**Modulus (Mpa)**	**Ethnicity**	**Age**	**Sex**
8	Left	103,635	11,259	White	58	Female
9	left	362,025	26,496	White	64	Male
9	Right	31,968	3,543	White	64	Male
10	Right	558,332	47,112	White	54	Male
11	Right	168,568	16,193	White	55	Male

Appendix II: Tables and Graphs

Table 1: Two sample t test for cadaver SS vs cadaver IS peak load (N)

Tests for equal means:

Cadaver SS		**Cadaver IS**	
N:	5	**N:**	5
Mean:	548,21	**Mean:**	432,57
95% conf.:	(223,93 872,49)	**95% conf.:**	(137,95 727,18)
Variance:	68208	**Variance:**	56300

Difference between means:	115,65
95% conf. interval (parametric):	(-248,24 479,53)
95% conf. interval (bootstrap):	(-159,46 389,21)

t :	0,733	**p (same mean):**	0,484

Table 2: Two sample t test for cadaver SS vs cadaver SC peak load (N)

Tests for equal means:

Cadaver SS		**Cadaver SC**	
N:	5	**N:**	4
Mean:	548,21	**Mean:**	452,04
95% conf.:	(223,93 872,49)	**95% conf.:**	(142,63 761,46)
Variance:	68208	**Variance:**	37811

Difference between means:	96,17
95% conf. interval (parametric):	(-276,44 468,77)
95% conf. interval (bootstrap):	(-155,99 357,68)

t :	0,610	**p (same mean):**	0,561

Table 3: Two sample t test for cadaver IS vs cadaver SC peak load (N)

Tests for equal means:

Cadaver IS		**Cadaver SC**	
N:	5	**N:**	4
Mean:	432,57	**Mean:**	452,04
95% conf.:	(137,95 727,18)	**95% conf.:**	(142,63 761,46)
Variance:	56300	**Variance:**	37811

Difference between means:	19,48
95% conf. interval (parametric):	(-329,4 368,36)
95% conf. interval (bootstrap):	(-227,64 258,88)

t :	-0,132	**p (same mean):**	0,899

Table 4: Two sample t test for bursal SS vs bursal IS peak load (N)

Tests for equal means

Bursal SS		**Bursal IS**	
N:	12	**N:**	12
Mean:	190,05	**Mean:**	171,13
95% conf.:	(104,19 275,91)	**95% conf.:**	(127,23 215,02)
Variance:	18260	**Variance:**	4772,9

Difference between means:	18,92
95% conf. interval (parametric):	(-71,937 109,78)
95% conf. interval (bootstrap):	(-65,741 101,6)

t :	0,432	**p (same mean):**	0,670

Table 5: Two sample t test for the bursal SS vs bursal SC peak load (N)

Tests for equal means:

Bursal SS		**Bursal SC**	
N:	12	**N:**	11
Mean:	190,05	**Mean:**	254,61
95% conf.:	(104,19 275,91)	**95% conf.:**	(137,73 371,49)
Variance:	18260	**Variance:**	30268

Difference between means:	64,56
95% conf. interval (parametric):	(-69,861 198,98)
95% conf. interval (bootstrap):	(-60,63 185,46)

t :	-0,999	**p (same mean):**	0,329

Table 6: Two sample t test for the bursal IS vs bursal SC peak load (N)

Tests for equal means:

Bursal IS		**Bursal SC**	
N:	12	**N:**	11
Mean:	171,13	**Mean:**	254,61
95% conf.:	(127,23 215,02)	**95% conf.:**	(137,73 371,49)
Variance:	4772,9	**Variance:**	30268

Difference between means:	83,48
95% conf. interval (parametric):	(-29,414 196,38)
95% conf. interval (bootstrap):	(-25,727 186,29)

t :	-1,538	**p (same mean):**	0,139

Table 7: Two sample t test for the capsular IS vs capsular SC peak load (N)

Tests for equal means:

Capsular IS		**Capsular SC**	
N:	4	**N:**	5
Mean:	203,94	**Mean:**	244,91
95% conf.:	(77,993 329,89)	**95% conf.:**	(-20,735 510,55)
Variance:	6265,2	**Variance:**	45770

Difference between means:	40,96
95% conf. interval (parametric):	(-228,41 310,33)
95% conf. interval (bootstrap):	(-143,75 211,19)

t :	-0,360	**p (same mean):**	0,730

Table 8: Two sample t test for the cadaver SC vs bursal SC peak load (N)

Tests for equal means:

Cadaver SC		**Bursal SC**	
N:	4	**N:**	11
Mean:	452,04	**Mean:**	254,61
95% conf.:	(142,63 761,46)	**95% conf.:**	(137,73 371,49)
Variance:	37811	**Variance:**	30268

Difference between means:	197,43
95% conf. interval (parametric):	(-28,241 423,11)
95% conf. interval (bootstrap):	(7,7894 387,05)

t :	1,890	**p (same mean):**	0,081

Table 9: Two sample t test for the cadaver IS vs capsular IS peak load (N)

Tests for equal means:

Cadaver IS		**Capsular IS**	
N:	5	**N:**	4
Mean:	432,57	**Mean:**	203,94
95% conf.:	(137,95 727,18)	**95% conf.:**	(77,993 329,89)
Variance:	56300	**Variance:**	6265,2

Difference between means:	228,62
95% conf. interval (parametric):	(-67,52 524,76)
95% conf. interval (bootstrap):	(42,815 434,82)

t :	1,826	**p (same mean):**	0,111

Table 10: Two sample t test for the cadaver SC vs capsular SC peak load (N)
Tests for equal means:

Cadaver SC		**Capsular SC**	
N:	4	**N:**	5
Mean:	452,04	**Mean:**	244,91
95% conf.:	(142,63 761,46)	**95% conf.:**	(-20,735 510,55)
Variance:	37811	**Variance:**	45770

Difference between means:	207,14
95% conf. interval (parametric):	(-119,32 533,6)
95% conf. interval (bootstrap):	(-17,35 444,18)

t :	1,500	**p (same mean):**	0,177

Table 11: Two sample t test for the bursal IS vs capsular IS peak load (N)
Tests for equal means:

Bursal IS		**Capsular IS**	
N:	12	**N:**	4
Mean:	171,13	**Mean:**	203,94
95% conf.:	(127,23 215,02)	**95% conf.:**	(77,993 329,89)
Variance:	4772,9	**Variance:**	6265,2

Difference between means:	32,81
95% conf. interval (parametric):	(-55,554 121,18)
95% conf. interval (bootstrap):	(-40,45 110,55)

t :	-0,796	**p (same mean):**	0,439

Table 12: Two sample t test for the bursal SC vs capsular SC peak load (N)
Tests for equal means:

Bursal SC		**Capsular SC**	
N:	11	**N:**	5
Mean:	254,61	**Mean:**	244,91
95% conf.:	(137,73 371,49)	**95% conf.:**	(-20,735 510,55)
Variance:	30268	**Variance:**	45770

Difference between means:	9,7052
95% conf. interval (parametric):	(-205,78 225,19)
95% conf. interval (bootstrap):	(-173,24 210,55)

t :	0,097	**p (same mean):**	0,924

Table 13: Two sample t test for the cadaver SS vs cadaver IS modulus (MPa)

Tests for equal means:

Cadaver SS		**Cadaver IS**	
N:	5	**N:**	3
Mean:	31,45	**Mean:**	47,23
95% conf.:	(17,283 45,624)	**95% conf.:**	(-65,763 160,23)
Variance:	130,24	**Variance:**	2069,1

Difference between means:	15,78
95% conf. interval (parametric):	(-34,016 65,577)
95% conf. interval (bootstrap):	(-34,347 50,14)

t :	-0,775	**p (same mean):**	0,468

Table 14: Two sample t test for the cadaver SS vs cadaver SC modulus (MPa)

Tests for equal means

A		**B**	
N:	5	**N:**	4
Mean:	31,45	**Mean:**	22,94
95% conf.:	(17,283 45,624)	**95% conf.:**	(-4,6215 50,491)
Variance:	130,24	**Variance:**	299,91

Difference between means:	8,52
95% conf. interval (parametric):	(-14,079 31,116)
95% conf. interval (bootstrap):	(-6,6734 26,729)

t :	0,891	**p (same mean):**	0,402
Uneq. var. t :	0,847	**p (same mean):**	0,435
Monte Carlo permutation:		**p (same mean):**	0,397
Exact permutation:		**p (same mean):**	0,405

Table 15: Two sample t test (test for equal means) – cadaver IS vs cadaver SC modulus (MPa)

Tests for equal means

A		**B**	
N:	3	**N:**	4
Mean:	47,23	**Mean:**	22,94
95% conf.:	(-65,763 160,23)	**95% conf.:**	(-4,6215 50,491)
Variance:	2069,1	**Variance:**	299,91

Difference between means:	24,30
95% conf. interval (parametric):	(-38,022 86,62)
95% conf. interval (bootstrap):	(-26,846 61,941)

t :	1,002	**p (same mean):**	0,362
Uneq. var. t :	0,879	**p (same mean):**	0,457
Monte Carlo permutation:		**p (same mean):**	0,456
Exact permutation:		**p (same mean):**	0,429

Table 16: Two sample t test (test for equal means) – bursal SS vs bursal IS modulus (MPa)

Tests for equal means

A		**B**	
N:	5	**N:**	5
Mean:	15,54	**Mean:**	11,53
95% conf.:	(5,903 25,167)	**95% conf.:**	(1,3781 21,678)
Variance:	60,18	**Variance:**	66,82

Difference between means:	4,01
95% conf. interval (parametric):	(-7,6147 15,629)
95% conf. interval (bootstrap):	(-4,35 13,257)

t :	0,795	**p (same mean):**	0,450
Uneq. var. t :	0,795	**p (same mean):**	0,450
Monte Carlo permutation:		**p (same mean):**	0,454
Exact permutation:		**p (same mean):**	0,452

Table 17: Two sample t test (test for equal means) – capsular SS vs capsular IS modulus (MPa)

Tests for equal means

A		**B**	
N:	4	**N:**	4
Mean:	27,41	**Mean:**	23,45
95% conf.:	(8,5709 46,243)	**95% conf.:**	(-3,6406 50,549)
Variance:	140,13	**Variance:**	289,94

Difference between means:	3,95
95% conf. interval (parametric):	(-21,419 29,325)
95% conf. interval (bootstrap):	(-12,526 21,733)

t :	0,381	**p (same mean):**	0,716
Uneq. var. t :	0,381	**p (same mean):**	0,718
Monte Carlo permutation:		**p (same mean):**	0,576
Exact permutation:		**p (same mean):**	0,571

Table 18: Two sample t test (test for equal means) – capsular SS vs capsular SC modulus (MPa)

Tests for equal means

A		**B**	
N:	4	**N:**	5
Mean:	27,41	**Mean:**	20,92
95% conf.:	(8,5709 46,243)	**95% conf.:**	(0,0072015 41,834)
Variance:	140,13	**Variance:**	283,69

Difference between means:	6,49
95% conf. interval (parametric):	(-17,156 30,129)
95% conf. interval (bootstrap):	(-9,9624 23,291)

t :	0,649	**p (same mean):**	0,537
Uneq. var. t :	0,677	**p (same mean):**	0,520
Monte Carlo permutation:		**p (same mean):**	0,534
Exact permutation:		**p (same mean):**	0,532

Table 19: Two sample t test (test for equal means) – capsular IS vs capsular SC modulus (MPa)

Tests for equal means

A		**B**	
N:	4	**N:**	5
Mean:	23,45	**Mean:**	20,92
95% conf.:	(-3,6406 50,549)	**95% conf.:**	(0,0072015 41,834)
Variance:	289,94	**Variance:**	283,69

Difference between means:	2,53
95% conf. interval (parametric):	(-24,309 29,376)
95% conf. interval (bootstrap):	(-17,237 21,38)

t :	0,223	**p (same mean):**	0,830
Uneq. var. t :	0,223	**p (same mean):**	0,830
Monte Carlo permutation:		**p (same mean):**	0,786
Exact permutation:		**p (same mean):**	0,786

Table 20: Two sample t test (test for equal means) – cadaver IS vs bursal IS modulus (MPa)

Tests for equal means

A		**B**	
N:	3	**N:**	5
Mean:	47,23	**Mean:**	11,53
95% conf.:	(-65,763 160,23)	**95% conf.:**	(1,3781 21,678)
Variance:	2069,1	**Variance:**	66,82

Difference between means:	35,71
95% conf. interval (parametric):	(-12,716 84,128)
95% conf. interval (bootstrap):	(-13,604 69,097)

t :	1,804	**p (same mean):**	0,121
Uneq. var. t :	1,347	**p (same mean):**	0,306
Monte Carlo permutation:		**p (same mean):**	0,020
Exact permutation:		**p (same mean):**	0,036

Table 21: Two sample t test (test for equal means) – cadaver SS vs capsular SS modulus (MPa)

Tests for equal means

A		**B**	
N:	5	**N:**	4
Mean:	31,45	**Mean:**	27,41
95% conf.:	(17,283 45,624)	**95% conf.:**	(8,5709 46,243)
Variance:	130,24	**Variance:**	140,13

Difference between means:	4,05
95% conf. interval (parametric):	(-14,348 22,441)
95% conf. interval (bootstrap):	(-8,4357 18,504)

t :	0,520	**p (same mean):**	0,619
Uneq. var. t :	0,518	**p (same mean):**	0,622
Monte Carlo permutation:		**p (same mean):**	0,594
Exact permutation:		**p (same mean):**	0,595

Table 22: Two sample t test (test for equal means) – cadaver IS vs capsular IS modulus (MPa)

Tests for equal means

A		**B**	
N:	3	**N:**	4
Mean:	47,23	**Mean:**	23,45
95% conf.:	(-65,763 160,23)	**95% conf.:**	(-3,6406 50,549)
Variance:	2069,1	**Variance:**	289,94

Difference between means:	23,78
95% conf. interval (parametric):	(-38,355 85,915)
95% conf. interval (bootstrap):	(-26,2 61,532)

t :	0,984	**p (same mean):**	0,370
Uneq. var. t :	0,861	**p (same mean):**	0,466
Monte Carlo permutation:		**p (same mean):**	0,457
Exact permutation:		**p (same mean):**	0,457

Table 23: Two sample t test (test for equal means) – cadaver SC vs capsular SC modulus (MPa)

Tests for equal means

A		**B**	
N:	4	**N:**	5
Mean:	22,94	**Mean:**	20,92
95% conf.:	(-4,6215 50,491)	**95% conf.:**	(0,0072015 41,834)
Variance:	299,91	**Variance:**	283,69

Difference between means:	2,01
95% conf. interval (parametric):	(-25,027 29,056)
95% conf. interval (bootstrap):	(-18,257 21,117)

t :	0,176	**p (same mean):**	0,865
Uneq. var. t :	0,176	**p (same mean):**	0,866
Monte Carlo permutation:		**p (same mean):**	0,825
Exact permutation:		**p (same mean):**	0,817

Table 24: Two sample t test (test for equal means) – bursal SS vs capsular SS modulus (MPa)

Tests for equal means

A		**B**	
N:	5	**N:**	4
Mean:	15,54	**Mean:**	27,41
95% conf.:	(5,903 25,167)	**95% conf.:**	(8,5709 46,243)
Variance:	60,18	**Variance:**	140,13

Difference between means:	11,87
95% conf. interval (parametric):	(-3,5428 27,287)
95% conf. interval (bootstrap):	(-0,6069 22,366)

t :	-1,821	**p (same mean):**	0,111
Uneq. var. t :	-1,731	**p (same mean):**	0,144
Monte Carlo permutation:		**p (same mean):**	0,119
Exact permutation:		**p (same mean):**	0,111

Table 25: Two sample t test (test for equal means) – bursal IS vs capsular IS modulus (MPa)

Tests for equal means

A		**B**	
N:	5	**N:**	4
Mean:	11,53	**Mean:**	23,45
95% conf.:	(1,3781 21,678)	**95% conf.:**	(-3,6406 50,549)
Variance:	66,82	**Variance:**	289,94

Difference between means:	11,93
95% conf. interval (parametric):	(-8,2907 32,143)
95% conf. interval (bootstrap):	(-5,6839 25,583)

t :	-1,395	**p (same mean):**	0,206
Uneq. var. t :	-1,287	**p (same mean):**	0,266
Monte Carlo permutation:		**p (same mean):**	0,212
Exact permutation:		**p (same mean):**	0,214

Table 26: Mann-Whitney u test (test for equal medians) – cadaver SS vs capsular SS peak load (N)

Tests for equal medians

Cadaver SS		**Capsular SS**	
N:	5	**N:**	4
Mean rank:	3,56	**Mean rank:**	1,44

Mann-Whitn U :	3		
z :	-1,592	**p (same med.):**	0,111

Table 27: Mann-Whitney u test (test for equal medians) – bursal SS vs capsular SS peak load (N)

Tests for equal medians

Bursal SS		**Capsular SS**	
N:	12	**N:**	4
Mean rank:	6,44	**Mean rank:**	2,06

Mann-Whitn U :	23		
z :	-0,060	**p (same med.):**	0,952

Table 28: Mann-Whitney u test (test for equal medians) – cadaver SC vs bursal SC modulus (MPa)

Tests for equal medians

A		B	
N:	4	N:	4
Mean rank:	1,63	Mean rank:	2,88

Mann-Whitn U :	3		
z :	-1,299	**p (same med.):**	0,194
Monte Carlo permutation:		**p (same med.):**	0,202
Exact permutation:		**p (same med.):**	0,2

Table 29: Mann-Whitney u test (test for equal medians) – bursal SC vs capsular SC modulus (MPa)

Tests for equal medians

A		**B**	
N:	4	**N:**	5
Mean rank:	3	**Mean rank:**	2

Mann-Whitn U :	3		
z :	-1,592	**p (same med.):**	0,111
Monte Carlo permutation:		**p (same med.):**	0,112
Exact permutation:		**p (same med.):**	0,111